UC Riverside
UC Riverside Previously Published Works

Title
Paternal USP26 mutations raise Klinefelter syndrome risk in the offspring of mice and humans

Permalink
https://escholarship.org/uc/item/6ns2k1cf

Journal
The EMBO Journal, 40(13)

ISSN
0261-4189

Authors
Liu, Chao
Liu, Hongbin
Zhang, Haobo
et al.

Publication Date
2021-07-01

DOI
10.15252/embj.2020106864

Peer reviewed

eScholarship.org Powered by the California Digital Library
University of California

Article

SOURCE DATA TRANSPARENT PROCESS

THE EMBO JOURNAL

Paternal *USP26* mutations raise Klinefelter syndrome risk in the offspring of mice and humans

Chao Liu[1,2,†], Hongbin Liu[3,4,†], Haobo Zhang[3,4,†], Lina Wang[1,5,†], Mengjing Li[3,4], Feifei Cai[3], Xiuge Wang[1,5], Li Wang[3,4], Ruidan Zhang[1,5], Sijie Yang[3,4], Wenwen Liu[1,5], Yu Liang[6], Liying Wang[1,5], Xiaohui Song[3,4], Shizhen Su[3,4], Hui Gao[1], Jing Jiang[7], Jinsong Li[7], Mengcheng Luo[8], Fei Gao[1,5], Qi Chen[9], Wei Li[1,2,5,*] & Zi-Jiang Chen[3,4,6,**]

Abstract

Current understanding holds that Klinefelter syndrome (KS) is not inherited, but arises randomly during meiosis. Whether there is any genetic basis for the origin of KS is unknown. Here, guided by our identification of some *USP26* variations apparently associated with KS, we found that knockout of *Usp26* in male mice resulted in the production of 41, XXY offspring. USP26 protein is localized at the XY body, and the disruption of *Usp26* causes incomplete sex chromosome pairing by destabilizing TEX11. The unpaired sex chromosomes then result in XY aneuploid spermatozoa. Consistent with our mouse results, a clinical study shows that some *USP26* variations increase the proportion of XY aneuploid spermatozoa in fertile men, and we identified two families with KS offspring wherein the father of the KS patient harbored a *USP26*-mutated haplotype, further supporting that paternal *USP26* mutation can cause KS offspring production. Thus, some KS should originate from XY spermatozoa, and paternal *USP26* mutations increase the risk of producing KS offspring.

Keywords infertility; Klinefelter syndrome; sex chromosome pairing; *USP26*; XY aneuploid spermatozoa

Subject Categories Cell Cycle; Development; Molecular Biology of Disease

DOI 10.15252/embj.2020106864 | Received 22 September 2020 | Revised 5 April 2021 | Accepted 16 April 2021

The EMBO Journal (2021) e106864

Introduction

Klinefelter syndrome (KS), which is defined by the 47, XXY karyotype, is the most frequent chromosome aberration in males and affects about 1 in 500–1,000 males (Groth *et al,* 2013). The prevalence of KS reaches to 3–4% among infertile males and is as high as 12% in azoospermic patients (Groth *et al,* 2013; Bonomi *et al,* 2017). The major signs and symptoms of KS include small, firm testes, gynecomastia, hypergonadotropic hypogonadism, and oligospermia or azoospermia (Lanfranco *et al,* 2004; Groth *et al,* 2013; Bonomi *et al,* 2017). Because only very small amounts of sperm can be found in around 50% adult KS patients' testicular tissue (Groth *et al,* 2013; Corona *et al,* 2017), most KS patients are infertile under physiological conditions (Groth *et al,* 2013; Bonomi *et al,* 2017; Corona *et al,* 2017). Knowledge about how to prevent or treat this disorder is urgently needed.

Since the 47, XXY karyotype was defined in KS patients in 1959, the pathology of KS has been found to be highly associated with X chromosome polysomy (Jacobs & Strong, 1959; Lanfranco *et al,* 2004; Groth *et al,* 2013). The presence of an extra X chromosome in KS might arise by non-disjunction during either meiosis I or meiosis II of maternal oogenesis or during meiosis I of paternal spermatogenesis (Thomas & Hassold, 2003; Lanfranco *et al,* 2004). Advanced maternal age is the only evidence-based risk factor for KS (Harvey *et al,* 1991; Tuttelmann & Gromoll, 2010), but because increased maternal age is a known strong etiological factor for other autosomal trisomies (Nicolaidis & Petersen, 1998), the maternal age-related cases of KS are likely similar to other autosomal trisomies. However, previous KS studies have shown that, in sharp contrast to

1 State Key Laboratory of Stem Cell and Reproductive Biology, Institute of Zoology, Stem Cell and Regenerative Medicine Innovation Institute, Chinese Academy of Sciences, Beijing, China
2 Fertility Preservation Lab, Reproductive Medicine Center, Guangdong Second Provincial General Hospital, Guangzhou, China
3 Center for Reproductive Medicine, Cheeloo College of Medicine, Key Laboratory of Reproductive Endocrinology of Ministry of Education, Shandong University, Jinan, China
4 Shandong Key Laboratory of Reproductive Medicine, Jinan, China
5 University of Chinese Academy of Sciences, Beijing, China
6 Shanghai Key Laboratory for Assisted Reproduction and Reproductive Genetics, Shanghai, China
7 Genome Tagging Project (GTP) Center, Shanghai Institute of Biochemistry and Cell Biology, Center for Excellence in Molecular Cell Science, Chinese Academy of Sciences, Shanghai, China
8 Department of Tissue and Embryology, School of Basic Medical Sciences, Wuhan University, Wuhan, China
9 Division of Biomedical Sciences, School of Medicine, University of California, Riverside, Riverside, CA, USA
*Corresponding author. Tel: +86 10 64807529; E-mail: leways@ioz.ac.cn
**Corresponding author. Tel: +86 531 85651188; Fax: +86 531 87068226; E-mail: chenzijiang@hotmail.com
†These authors contributed equally to this work

© 2021 The Authors

most of the autosomal trisomies that largely originate from maternal meiotic defects (90%), the extra X chromosome in KS is equally likely to be of maternal or paternal origin (Hassold & Hunt, 2001; Thomas & Hassold, 2003). The fathers of KS patients also produce higher frequencies of XY sperm (Lowe *et al,* 2001; Eskenazi *et al,* 2002), highlighting that KS has a strong tendency for paternal origin among trisomy disorders. Further, although impaired recombination between paternal sex chromosomes in the pseudoautosomal region (PAR) during meiosis I has been proposed as a major cause of paternal-origin KS (Hassold *et al,* 1991; Thomas *et al,* 2000), the molecular mechanisms underlying the origin of KS are still largely unknown.

Here, we conducted a genetic analysis using whole-exome sequencing (WES) in 108 unrelated KS patients and identified *USP26* germline mutations that might be responsible for promoting paternal-origin KS (Fig 1). *USP26* has been associated with nonobstructive azoospermia (Xia *et al,* 2014; Luddi *et al,* 2016; Ma *et al,* 2016; Arafat *et al,* 2020), and *Usp26* knockout mouse models only display a very slight impact on male fertility (Felipe-Medina *et al,* 2019; Sakai *et al,* 2019; Tian *et al,* 2019). While we found that 2-month-old $Usp26^{-/Y}$ mice were indeed fertile, both the pregnancy rates and the litter sizes of $Usp26^{-/Y}$ mice were significantly reduced with increasing age (6-month-old mice; Fig 2A–D). Further investigation showed the knockout of *Usp26* in male mice impaired sex chromosome pairing by destabilizing TEX11, which resulted in XY aneuploid spermatozoa and ultimately produced 41, XXY offspring. In fertile men, some *USP26* variations increased the proportion of XY aneuploid spermatozoa, and we found that the father of two KS patients harbored a *USP26*-mutated haplotype. Although the deficiency of paternal *Usp26* does not invariably result in the production of XXY progeny mice (or KS children for the mutated haplotype), *Usp26* deletion or the mutated haplotype does greatly increase the overall frequency of KS offspring production.

Results

Whole-genome sequencing-based mutational scanning in KS patients

To study the potential genetic basis for paternal-origin KS, we performed WES in 108 unrelated KS patients with the classical 47, XXY karyotype (1st cohort; Fig 1A and B). A total of 179,579 sequence variants were identified in the KS subset, and we subsequently investigated the nonsense, missense, frameshift, and splice-site variants among them (Fig 1C, Dataset EV1 and Table EV1). These variants were divided into four subtypes according to their frequencies, genomic localization, and potential deleterious effects (Fig 1C). Briefly, it was notable that many of the predicted deleterious variants were localized on the X chromosome (Fig 1C and D), and recalling that KS is the trisomy disorder for which paternal origin is most prevalent, and our interest was piqued by *USP26* (Fig 1E and F, Table EV2), a gene for which multiple variants were detected in this cohort and which was previously reported to have a strictly testis-specific expression pattern (Wang *et al,* 2001).

Our WES data showed six variations of *USP26* in 29 of the 108 KS patients. Extending this inquiry, we sequenced the coding regions of *USP26* in an additional 354 KS patients and in 272 fertile men (Table EV1 and Table EV3), which led to our identification of *USP26* variants in 49 KS patients, including two synonymous mutations in 2 KS patients, three missense mutations in 12 KS patients, and a mutated haplotype in 35 KS patients. Moreover, we found that the c.191A>G[p.Y64C], c.313G>A[p.E105K], c.1030C>T[p.R344W], and c.1691A>T[p.D564V] variants only occurred in the KS patients. Thus, the *USP26* variants appeared likely to impact the etiology of KS origin.

XXY offspring production from Usp26-deficient mice

USP26 belongs to a family of ubiquitin-specific proteases that remove ubiquitin chains from substrates (Dirac & Bernards, 2010; Lahav-Baratz *et al,* 2017; Ning *et al,* 2017), and *USP26* has been reported to be associated with nonobstructive azoospermia, while others have found contradictory results, and thus, this association remains debatable (Xia *et al,* 2014; Zhang *et al,* 2015; Luddi *et al,* 2016; Ma *et al,* 2016). To determine whether *USP26* mutations lead to KS offspring, we generated *Usp26*-knockout mice using the CRISPR-Cas9 system (Fig 2A). As *Usp26* localized on the X chromosome, the *Usp26* knockout male mice were called $Usp26^{-/Y}$. We first measured the knockout efficiency and found that the USP26 protein was completely depleted in $Usp26^{-/Y}$ testes (Fig 2B), indicating that the knockout mice were *Usp26*-null. The $Usp26^{-/Y}$ mice were viable and reached adulthood without any observable defects. We observed age-related phenotypes for fertility in $Usp26^{-/Y}$ mice: Both the pregnancy rate and litter size of $Usp26^{-/Y}$ mice were significantly reduced with increasing age (Fig 2C and D). It was highly

Figure 1. *USP26* variants might be responsible for the origin of Klinefelter syndrome.

A The karyotype of KS patients and controls.

B The cohorts used in this study. The first cohort that contained 108 unrelated KS patients with the classical 47, XXY karyotype was selected to perform WES, the second cohort that contained 354 unrelated KS patients was selected to perform Sanger sequencing in the coding regions of *USP26*, and the third cohort that contained 558 unrelated KS patients was selected to perform Sanger sequencing in the mutated haplotype (c.370–371insACA/494T>C/1423C>T) of *USP26*.

C WES data analysis pipeline. A total of 179,579 sequence variants in 20,800 genes were identified in 108 unrelated KS patients, and among them nonsense, missense, frameshift, and essential splice-site variants were further investigated. These variants were divided into four subtypes (high, likely high, medium, and low), and most of the medium to high variants were localized on the X chromosome. The genes on the X chromosome that contained more than two types of medium to high variants were selected. As the extra paternal-origin X chromosome in KS might be caused by impaired recombination between sex chromosomes during meiosis I, only the testis-specific genes *ESX1*, *LOC101059915*, and *USP26* were further investigated. The variant frequencies of these three genes in the KS patients were compared with the variant frequencies of these three genes in the 1000 Genomes Project. The frequency of *USP26* variants had the highest fold increase.

D The genomic localization of sequence variants in 108 KS patients.

E Genes with more than two medium- to high-level variants on the X chromosome. The testis-specific genes are labeled in red.

F The frequency difference between KS patients and the 1000 Genomes Project.

 © 2021 The Authors

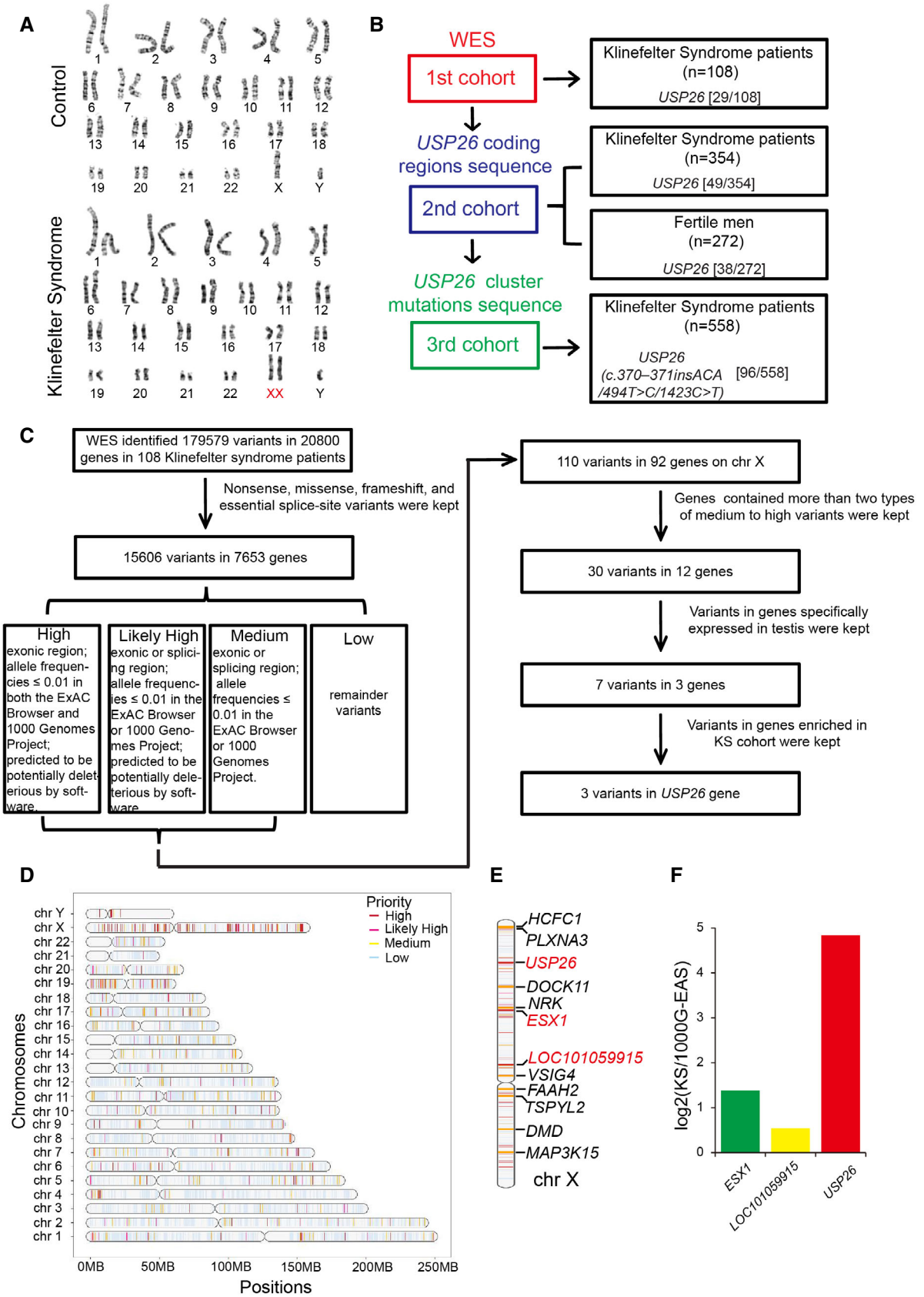
A
Control
Klinefelter Syndrome
XX
B
WES
1st cohort
Klinefelter Syndrome patients (n=108)
USP26 [29/108]
USP26 coding regions sequence
2nd cohort
Klinefelter Syndrome patients (n=354)
USP26 [49/354]
Fertile men (n=272)
USP26 [38/272]
USP26 cluster mutations sequence
3rd cohort
Klinefelter Syndrome patients (n=558)
USP26 (c.370–371insACA /494T>C/1423C>T) [96/558]
C
WES identified 179579 variants in 20800 genes in 108 Klinefelter syndrome patients
Nonsense, missense, frameshift, and essential splice-site variants were kept
15606 variants in 7653 genes
High
exonic region; allele frequencies ≤ 0.01 in both the ExAC Browser and 1000 Genomes Project; predicted to be potentially deleterious by software.
Likely High
exonic or splicing region; allele frequencies ≤ 0.01 in the ExAC Browser or 1000 Genomes Project; predicted to be potentially deleterious by software
Medium
exonic or splicing region; allele frequencies ≤ 0.01 in the ExAC Browser or 1000 Genomes Project.
Low
remainder variants
110 variants in 92 genes on chr X
Genes contained more than two types of medium to high variants were kept
30 variants in 12 genes
Variants in genes specifically expressed in testis were kept
7 variants in 3 genes
Variants in genes enriched in KS cohort were kept
3 variants in USP26 gene
D
Priority
High
Likely High
Medium
Low
Chromosomes
Positions
0MB
50MB
100MB
150MB
200MB
250MB
E
HCFC1
PLXNA3
USP26
DOCK11
NRK
ESX1
LOC101059915
VSIG4
FAAH2
TSPYL2
DMD
MAP3K15
chr X
F
log2(KS/1000G-EAS)
ESX1
LOC101059915
USP26

Figure 1.

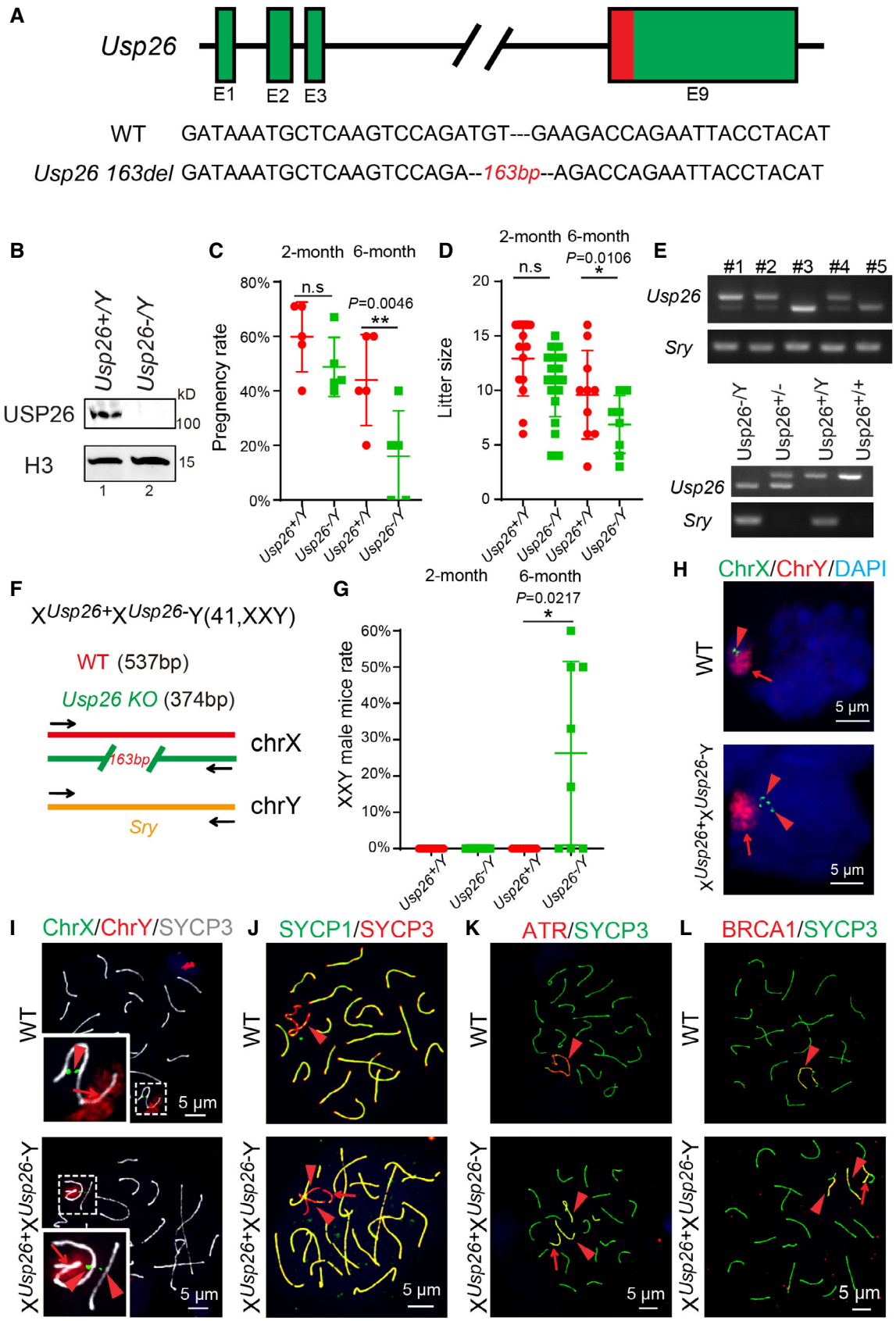

Figure 2.

© 2021 The Authors

Figure 2. *Usp26*-deficient mice produce 41, XXY offspring.

A Sequences of the WT and *Usp26* mutant alleles in mice.

B The USP26 protein was absent in $Usp26^{-/Y}$ testes. Immunoblotting of USP26 was performed in $Usp26^{+/Y}$ and $Usp26^{-/Y}$ testes. Histone 3 served as the loading control.

C, D The fertility of $Usp26^{-/Y}$ mice was reduced with increasing age. The fertility assessment experiments were performed in 2-month-old $Usp26^{+/Y}$, $Usp26^{-/Y}$ mice (n = 5 independent experiments) and 6-month-old $Usp26^{+/Y}$, $Usp26^{-/Y}$ mice (n = 5 independent experiments) (C). The litter sizes were observed in 2-month-old $Usp26^{+/Y}$, $Usp26^{-/Y}$ mice (n = 14, 22 independent experiments for $Usp26^{+/Y}$ and $Usp26^{-/Y}$, respectively) and 6-month-old $Usp26^{+/Y}$, $Usp26^{-/Y}$ mice (n = 10, 8 independent experiments for $Usp26^{+/Y}$ and $Usp26^{-/Y}$, respectively) (D). Red dots indicate $Usp26^{+/Y}$ mice, and green dots indicate $Usp26^{-/Y}$ mice.

E Genotyping of $Usp26^{-/Y}$ mice offspring. The upper subpanel indicates the genotyping of $Usp26^{-/Y}$ mice male offspring by using *Usp26* and *Sry* primers. The lower subpanel indicates the genotyping of $Usp26^{-/Y}$, $Usp26^{+/Y}$ male mice and $Usp26^{+/-}$, $Usp26^{+/+}$ female mice by using *Usp26* and *Sry* primers.

F The wild-type (WT) and *Usp26* knock out alleles in $X^{Usp26+}X^{Usp26-}Y$ mice.

G The proportion of 41, XXY mice among the male offspring of 2-month-old $Usp26^{+/Y}$, $Usp26^{-/Y}$ and 6-month-old $Usp26^{+/Y}$, $Usp26^{-/Y}$ mice (n = 14, 22, 10, and 8 independent experiments for the offspring of 2-month-old $Usp26^{+/Y}$, $Usp26^{-/Y}$ mice, 6-month-old $Usp26^{+/Y}$, and $Usp26^{-/Y}$ mice, respectively). Red dots indicate $Usp26^{+/Y}$ mice, and green dots indicate $Usp26^{-/Y}$ mice.

H, I Two pair of X chromosomes could be detected in the 2-month-old $X^{Usp26+}X^{Usp26-}Y$ spermatocytes. FISH analysis of Chr X-FISH (green) and Chr Y-FISH (red) was performed in WT and $X^{Usp26+}X^{Usp26-}Y$ spermatocytes (H). Immunofluorescence analysis of Chr X-FISH (green), Chr Y-FISH (red), and SYCP3 (white) was performed in WT and $X^{Usp26+}X^{Usp26-}Y$ spermatocytes (I). The arrows indicate the Y chromosome, and the arrowheads indicate the X chromosome. Nuclei were stained with DAPI (blue).

J–L Three sex chromosome axes could be detected in the 2-month-old $X^{Usp26+}X^{Usp26-}Y$ spermatocytes. Immunofluorescence analysis of SYCP3 (red) and SYCP1 (green) in (J), ATR (red) and SYCP3 (green) in (K) and BRCA1 (red) and SYCP3 (green) in (L) was performed in 2-month-old WT and $X^{Usp26+}X^{Usp26-}Y$ spermatocytes. Nuclei were stained with DAPI (blue). The arrows indicate the Y chromosome. The arrowheads indicate the X chromosome.

Data information: In (C), (D), and (G), data are presented as mean ± SD. *P < 0.05, **P < 0.01 (Student's t-test). n.s, not significant. Numerical source data for panels (C)/(D)/(G) can be found in Table EV5.
Source data are available online for this figure.

conspicuous that 2-month-old $Usp26^{-/Y}$ mice did not produce XXY mice, but approximately 20% of the male mice sired by 6-month-old $Usp26^{-/Y}$ fathers were XXY (Fig 2E–G). We also found that the proportion of XXY offspring sired by 6-month-old $Usp26^{-/Y}$ male mice was highly variable (Fig 2G). In some cases, there were no XXY male offspring, while some litters showed more than 50% rate with XXY males (Fig 2G). Thus, the disruption of *Usp26* does not absolutely result in the production of XXY mice in their offspring.

As most KS patients and reported XXY mouse models show azoospermia (Swerdloff *et al,* 2011; Groth *et al,* 2013), we analyzed spermatogenesis in these $X^{Usp26+}X^{Usp26-}Y$ mice, which were the offspring of the $Usp26^{-/Y}$ mice. We found that $X^{Usp26+}X^{Usp26-}Y$ mice had significantly reduced testis size and weight (Fig EV1A and B), and histological examination by hematoxylin and eosin staining showed that most of the $X^{Usp26+}X^{Usp26-}Y$ testes lacked post-meiotic cells (Fig EV1C–E). To identify which stages of spermatogenesis were affected in $X^{Usp26+}X^{Usp26-}Y$ mice, Periodic Acid-Schiff (PAS) and hematoxylin staining was performed. Some dead pachytene and metaphase spermatocytes were identified in the seminiferous tubules of $X^{Usp26+}X^{Usp26-}Y$ mice (Fig EV1E), indicating that many of the $X^{Usp26+}X^{Usp26-}Y$ spermatocytes might be arrested at the pachytene and meiotic division stages. Although few $X^{Usp26+}X^{Usp26-}Y$ spermatocytes could go through the meiotic division, the spermatid differentiation was blocked in $X^{Usp26+}X^{Usp26-}Y$ mice, resulting in the absence of mature spermatozoa (Fig EV1C–E), which is a similar phenotype as KS patients (Lanfranco *et al,* 2004; Groth *et al,* 2013; Bonomi *et al,* 2017).

We then examined the sex chromosomes in the $X^{Usp26+}X^{Usp26-}Y$ mouse spermatocytes using fluorescent in situ hybridization (FISH) of X and Y chromosomes. Four signals of the X chromosome probe could be detected in the $X^{Usp26+}X^{Usp26-}Y$ spermatocytes (Fig 2H and I), each of the two X probe signals originates from one sister chromatid, indicating that they were indeed 41, XXY male mice. Furthermore, three unsynapsed sex chromosome axes could be detected in the $X^{Usp26+}X^{Usp26-}Y$ spermatocytes (Fig 2J), and the staining for ATR and BRCA1, which localize on the sex chromosome axes in the pachytene stage (Lu *et al,* 2013), showed three sex chromosome axes in the $X^{Usp26+}X^{Usp26-}Y$ spermatocytes but only two axes in control littermates (Fig 2K and L). Thus, we conclude that the production of 41, XXY offspring increases with aging in $Usp26^{-/Y}$ male mice.

Impaired sex chromosome pairing in $Usp26^{-/Y}$ mice

The disruption of *Usp26* in mice caused male subfertility, which is similar to a recent report (Tian *et al,* 2019). To further determine the effect of *Usp26* knockout, we analyzed the process of spermatogenesis in 6-month-old $Usp26^{-/Y}$ mice and found significantly decreases in testis size and weight in the $Usp26^{-/Y}$ mice (Fig 3A–C). We also observed two distinct types of seminiferous tubules in the 6-month-old $Usp26^{-/Y}$ mice one type showing normal tubule structure and the other type showing a disorganized structure and featuring large vacuoles and apoptotic cells (Fig 3D). Moreover, the total number of spermatozoa was reduced in 6-month-old $Usp26^{-/Y}$ mice compared with 6-month-old $Usp26^{+/Y}$ mice, and fewer spermatozoa were detected in the cauda epididymis of $Usp26^{-/Y}$ mice (Fig 3D and E). These results indicate that disruption of *Usp26* impairs spermatogenesis to some extent.

We used PAS and hematoxylin staining to identify which stages of spermatogenesis were affected in 6-month-old $Usp26^{-/Y}$ mice: Dead pachytene and metaphase spermatocytes were found at stages IV and XII in the impaired seminiferous tubules of $Usp26^{-/Y}$ mice (Fig 3F). TUNEL-positive (i.e., apoptotic) signals were detected in the pachytene and metaphase spermatocytes in testes from 6-month-old $Usp26^{-/Y}$ but not from $Usp26^{+/Y}$ mice (Figs 5D and EV2A–C), suggesting that disruption of *Usp26* might cause pachytene and meiotic division arrest.

We used immunoblotting of various mouse organs to explore the physiological function of USP26 and found that USP26 was predominantly expressed in the testis (Fig 4A), although some low-

© 2021 The Authors

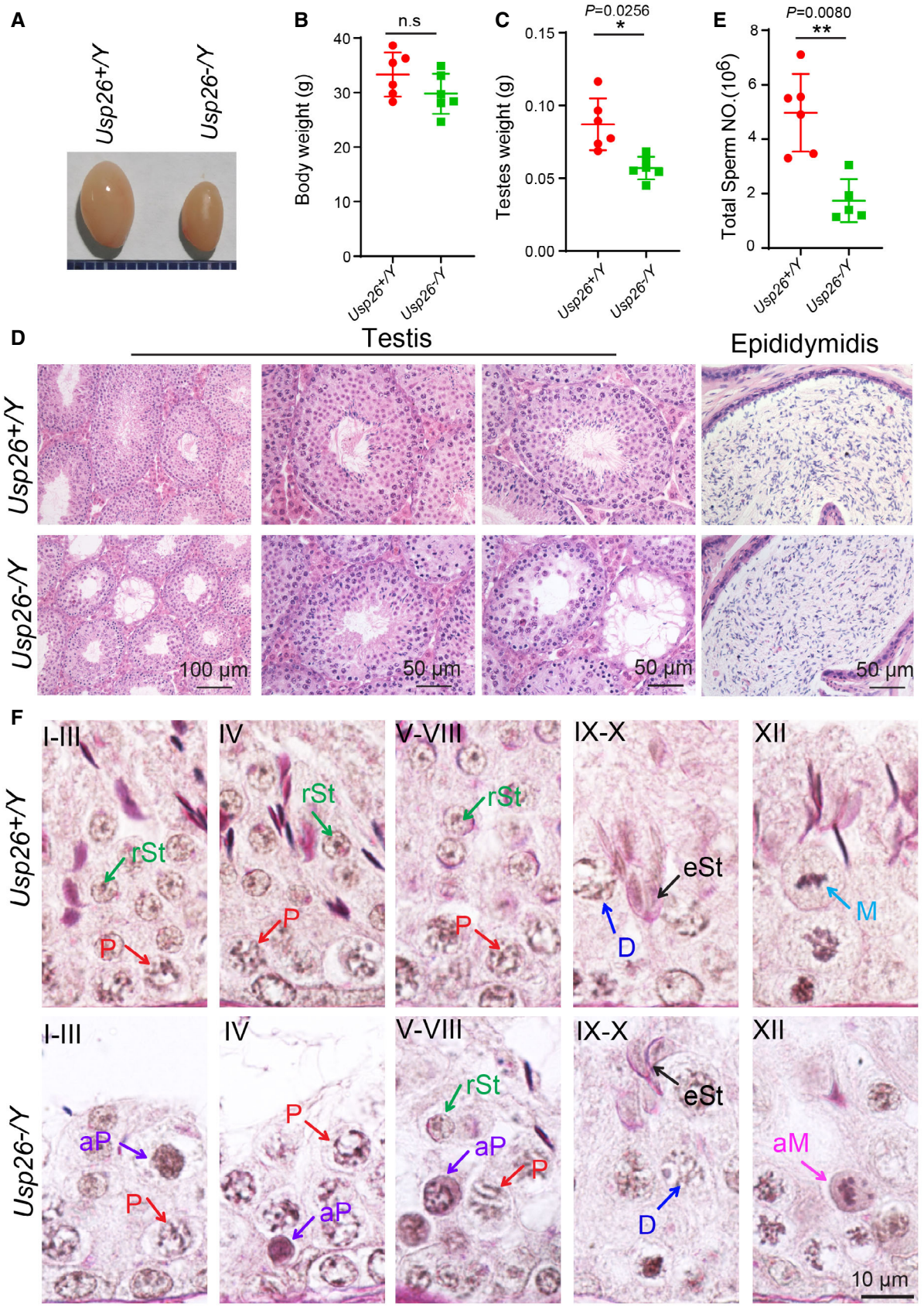

Figure 3.

© 2021 The Authors

Figure 3. The disruption of *Usp26* impairs spermatogenesis.

A The size of the testes was smaller in the 6-month-old $Usp26^{-/Y}$ mice.

B Quantification of body weight in 6-month-old $Usp26^{+/Y}$ and $Usp26^{-/Y}$ mice (n = 6 independent experiments). P = 0.2442. Red dots indicate $Usp26^{+/Y}$ mice, and green dots indicate $Usp26^{-/Y}$ mice.

C Quantification of testis weight in 6-month-old $Usp26^{+/Y}$ and $Usp26^{-/Y}$ mice (n = 6 independent experiments). Red dots indicate $Usp26^{+/Y}$ mice, and green dots indicate $Usp26^{-/Y}$ mice.

D Histological analysis of the seminiferous tubules and caudal epididymis of the 6-month-old $Usp26^{+/Y}$ and $Usp26^{-/Y}$ mice.

E The sperm counts in the caudal epididymis were measured in 6-month-old $Usp26^{+/Y}$ and $Usp26^{+/-/Y}$ mice (n = 6 and 5 independent experiments for $Usp26^{+/Y}$ and $Usp26^{-/Y}$, respectively). Red dots indicate $Usp26^{+/Y}$ mice, and green dots indicate $Usp26^{-/Y}$ mice.

F The deletion of *Usp26* causes pachytene and meiotic division arrest. Representative PAS-hematoxylin staining in 6-month-old $Usp26^{+/Y}$ and $Usp26^{-/Y}$ seminiferous tubules. Paraffin sections from $Usp26^{+/Y}$ and $Usp26^{-/Y}$ testes were stained with PAS-hematoxylin. aM, abnormal meiotic divisions; aP, apoptotic pachytene spermatocyte; D, diplotene spermatocyte; eST, elongating spermatid; M, meiotic spermatocyte; P, pachytene spermatocyte; rST, round spermatid.

Data information: In (B), (C), and (E), data are presented as mean ± SD. *P < 0.05, **P < 0.01 (Student's t-test). n.s, not significant. Numerical source data for panels (B)/(C)/(E) can be found in Table EV5.

molecular-weight protein isoforms or degradation forms could be observed in other organs. We then characterized its precise localization during spermatogenesis by immunostaining spread nuclei and found that USP26 appeared along with the synapsed chromosome axes in the early-pachytene stage. The signal was predominantly localized on the XY body region in the late-pachytene and diplotene stages (Fig 4B), suggesting that USP26 participates in sex chromosome recombination and synapsis.

When we examined homologous chromosomes synapsis, we noted that the sex chromosomes failed to synapse in some 6-month-old $Usp26^{-/Y}$ spermatocytes (Fig 4C and D). To further confirm this observation, we performed FISH of the X and Y chromosomes and found that about 2% of WT spermatocytes had unpaired sex chromosomes at this stage, while around 40% of sex chromosomes were unpaired in 6-month-old $Usp26^{-/Y}$ spermatocytes we examined (Fig 4E and F).

During meiosis, the pairing and synapsis of the X and Y chromosome is thought to be dependent on the introduction of DNA double-strand breaks (DSBs) and further recombination on the sex chromosomes (Barchi *et al,* 2008; Kauppi *et al,* 2011; Acquaviva *et al,* 2020). Therefore, we first analyzed the efficiency of DSB formation in 6-month-old $Usp26^{-/Y}$ spermatocytes and found that MRE11 and γH2AX—which are required for regulating programmed DSB formation (Wang *et al,* 2005; Cherry *et al,* 2007)—were detectable at the leptotene and zygotene stages (Fig 4G and H), suggesting that DSBs were produced independently of USP26. At the pachytene stage, MRE11 and γH2AX persisted only on sex chromosomes, and both of these proteins appeared on the XY body in wild-type spermatocytes but their signals were clearly fragmented from the XY body of the $Usp26^{-/Y}$ spermatocytes (Fig 4G and H). p-ATM, which is essential for meiotic programmed DSB formation (Wang *et al,* 2005), was also detected exclusively on the sex chromosomes of $Usp26^{-/Y}$ spermatocytes (Fig 4I). These results indicate that induced DSBs can form on both autosomal and sex chromosomes of $Usp26^{-/Y}$ spermatocytes and that disruption of *Usp26* has no effect on autosomal DSB repair. We next monitored the DSB repair process on the sex chromosomes by staining for the meiosis-specific recombination-related protein, DMC1 (Neale & Keeney, 2006). At the pachytene stage of $Usp26^{-/Y}$ spermatocytes, the number of DMC1 foci was dramatically increased, especially on the sex chromosomes (Fig 4J and K), indicating that the meiotic DSBs on the sex chromosomes are persistently produced or that DSB repair

Figure 4. USP26 participates in sex chromosome pairing.

A USP26 was predominately expressed in the testis. Immunoblotting of USP26 was performed in the heart, liver, spleen, lung, kidney, intestine, brain, ovary, and testis. Histone 3 served as the loading control.

B The localization of USP26 during meiosis. Immunofluorescence analysis of SYCP3 (red) and USP26 (white) was performed in wild-type spermatocytes. Nuclei were stained with DAPI (blue). The circles indicate the XY body.

C, D The sex chromosomes failed to synapse in the 6-month-old *Usp26*-deficient spermatocytes. Immunofluorescence analysis of SYCP3 (green), ATR (white), SYCP1 (red) (C); SYCP3 (green), ATR (white), and TRF1 (red) (D) was performed in 6-month-old $Usp26^{+/Y}$ and $Usp26^{-/Y}$ spermatocytes. Nuclei were stained with DAPI (blue). The arrows indicate the sex chromosomes.

E The X and Y chromosomes were unpaired in $Usp26^{-/Y}$ spermatocytes. Immunofluorescence analysis of Chr X-FISH (green), Chr Y-FISH (red), and SYCP3 (white) was performed in 6-month-old $Usp26^{+/Y}$ and $Usp26^{-/Y}$ spermatocytes. The arrowheads indicate the X chromosome.

F Quantification of unpaired X and Y chromosomes in 6-month-old $Usp26^{+/Y}$ and $Usp26^{-/Y}$ mice (n = 5 independent experiments). Red dots indicate $Usp26^{+/Y}$ mice, and green dots indicate $Usp26^{-/Y}$ mice.

G–J Sex chromosome recombination was perturbed in 6-month-old $Usp26^{-/Y}$ mice. Immunofluorescence analysis of SYCP3 (green), MRE11 (red) (G); SYCP3 (green), γH2AX (red) (H); SYCP3 (green), ATR (red), p-ATM (pink) (I); DMC1 (green), SYCP3 (red) (J) was performed in 6-month-old $Usp26^{+/Y}$ and $Usp26^{-/Y}$ spermatocytes. Nuclei were stained with DAPI (blue). The arrows indicate the sex chromosomes.

K Quantification of the numbers of DMC1 foci in 6-month-old $Usp26^{+/Y}$ (n = 50, zygotene, n = 31, early-pachytene) and $Usp26^{-/Y}$ (n = 31, zygotene, n = 24, early-pachytene) spermatocytes. P = 0.1893 for Zygotene. Red dots indicate $Usp26^{+/Y}$ mice, and green dots indicate $Usp26^{-/Y}$ mice.

L Crossover on sex chromosomes was impaired in 6-month-old $Usp26^{-/Y}$ mice. Immunofluorescence analysis of SYCP3 (red), MLH1 (green), and ATR (white) was performed in 6-month-old $Usp26^{+/Y}$ and $Usp26^{-/Y}$ spermatocytes. Nuclei were stained with DAPI (blue).

Data information: In (F) and (K), data are presented as mean ± SD. **P < 0.01 (Student's t-test). n.s, not significant. Numerical source data for panels (F)/(K) can be found in Table EV5.
Source data are available online for this figure.

© 2021 The Authors

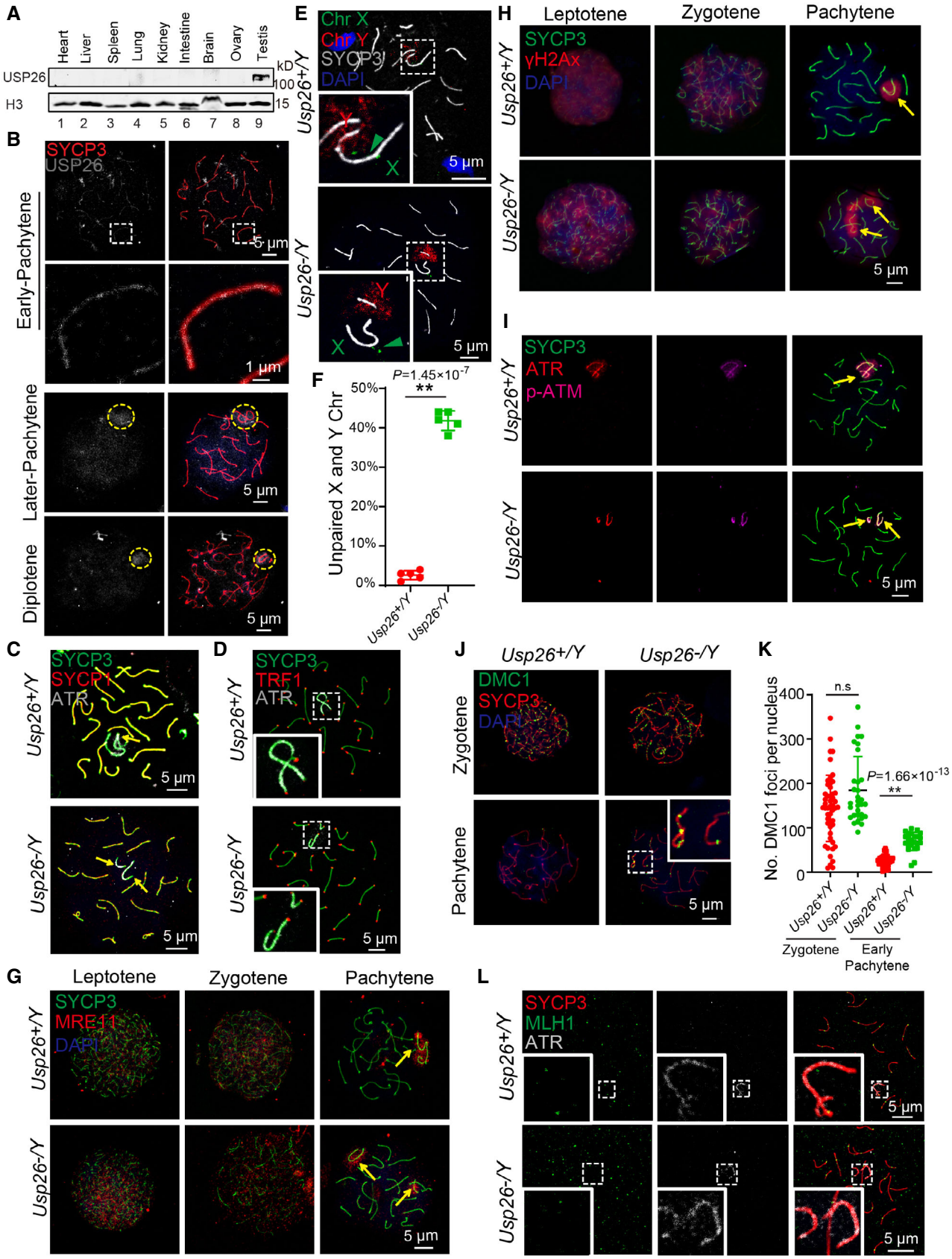

Figure 4.

© 2021 The Authors

intermediates are not resolved in a timely manner in *Usp26*$^{-/Y}$ spermatocytes. The majority of DSB repair intermediates are typically resolved before crossover formation occurs, which can be observed using the crossover marker protein MLH1 (Baker *et al*, 1996; Moens *et al*, 2002), and we found that crossover formation on the sex chromosomes was impaired in *Usp26*$^{-/Y}$ spermatocytes (Fig 4L). Therefore, our results support that USP26 is essential for the synapsis of the sex chromosomes.

During meiosis, transcription from the sex chromosomes is suppressed at mid-pachytene in the XY body in a process termed meiotic sex chromosome inactivation (MSCI), and failure of MSCI often causes the sex chromosomes to fall apart, leading to spermatocyte death (Turner, 2007; Lu & Yu, 2015). To test whether the unpaired sex chromosomes in 6-month-old *Usp26*$^{-/Y}$ spermatocytes are impacted by MSCI, we examined several MSCI-related proteins (*e.g.*, MDC1, ATR, BRCA1, and UbH2A (Turner, 2007)) in 6-month-old *Usp26*$^{-/Y}$ and *Usp26*$^{+/Y}$ spermatocytes. All of these proteins were detected on the sex chromosomes of both *Usp26*$^{-/Y}$ and *Usp26*$^{+/Y}$ spermatocytes (Figs 4I and EV2D–F), indicating that the disruption of *Usp26* might have no effect on MSCI. We also evaluated the localization of RNA polymerase II (Pol II) in 6-month-old *Usp26*$^{-/Y}$ and *Usp26*$^{+/Y}$ spermatocytes (Fig EV2G). Similar to the control group, the transcription machinery was excluded from the XY body in *Usp26*$^{-/Y}$ spermatocytes (Fig EV2G). Taken together, the disruption of *Usp26* may impair the resolution of DSB repair intermediates, which would disrupt subsequent crossover formation on the sex chromosomes. Unpaired sex chromosomes could also be detected in 6-month-old *Usp26*-16bp-deletion and *Usp26*-2664bp-deletion mice (Fig EV3), indicating that this is common phenotype for all kinds of *Usp26*-null male mice.

The unpaired sex chromosomes in *Usp26*-deficient mice produce XY aneuploid spermatozoa

Because chromosome pairing and synapsis are essential for correct homolog alignment at metaphase of meiosis I, errors in meiotic recombination and chromosome synapsis may increase the possibility that cells progress to metaphase with univalent chromosomes. Further, the unpaired sex chromosomes observed in 6-month-old *Usp26*$^{-/Y}$ spermatocytes may cause mis-segregation in metaphase I. Indeed, we observed a significant increase in the proportion of 6-month-old *Usp26*$^{-/Y}$ spindles with laggard chromosomes as compared to *Usp26*$^{+/Y}$ spermatocytes (Fig 5A–C), indicating that the deletion of *Usp26* causes unpaired sex chromosomes and further leads to univalent chromosomes in metaphase I. Non-exchanged chromosomes are usually monitored in cells by tracking the spindle assembly checkpoint (SAC) protein, which is known to trigger cell death (Sun & Kim, 2012). However, when we assessed apoptosis via TUNEL staining, we found that some *Usp26*-deficient metaphase I spermatocytes with laggard chromosomes stained negative (Fig 5D), suggesting that these *Usp26*$^{-/Y}$ spermatocytes with mis-segregated sex chromosomes can somehow escape from the apoptosis-triggering function of the SAC. To further confirm this, we detected reductions in the levels of three known spindle assembly checkpoint-related proteins in 6-month-old *Usp26*$^{-/Y}$ mice compared with *Usp26*$^{+/Y}$ mice (Fig 5E), while not in 2-month-old *Usp26*$^{-/Y}$ mice (Fig 5E).

In theory, if the sex chromosomes randomly segregated at meiosis I, the spermatozoa would have 25% distributions of X, Y, XY, and O spermatozoa. We first examined the X and Y chromosomes in round spermatids and found that, with increasing age, a significantly higher proportion of XY and O aneuploid round spermatids

Figure 5. *Usp26*-deficient mice produce XY aneuploid spermatozoa.

A, B Laggard chromosomes were observed in the metaphase I of 6-month-old *Usp26*$^{-/Y}$ spermatocytes. Immunofluorescence analysis of tubulin (green) was performed in 6-month-old *Usp26*$^{+/Y}$ and *Usp26*$^{-/Y}$ spermatocytes. Nuclei were stained with DAPI (blue). The arrowheads indicate the laggard chromosomes.

C The proportion of metaphase I spermatocytes exhibiting laggard chromosomes in 6-month-old *Usp26*$^{+/Y}$ and *Usp26*$^{-/Y}$ mice spermatocytes (n = 5 independent experiments). Red dots indicate *Usp26*$^{+/Y}$ mice, and green dots indicate *Usp26*$^{-/Y}$ mice.

D Representative TUNEL results in *Usp26*$^{+/Y}$ and *Usp26*$^{-/Y}$ testes. Paraffin sections from 6-month-old *Usp26*$^{+/Y}$ and *Usp26*$^{-/Y}$ testes were stained with TUNEL (green) and DAPI (blue) to show dead cells in stage IV, VIII, and XII tubules with pachytene spermatocytes, round spermatids, and metaphase spermatocytes, respectively. The arrowheads indicate the laggard chromosomes. aM, abnormal meiotic divisions; aP, apoptotic pachytene spermatocyte; arSt, apoptotic round spermatid; M, meiotic spermatocyte; P, pachytene spermatocyte; rSt, round spermatid; spz, spermatozoa.

E The protein level of three known SAC proteins was detected in 2-month-old and 6-month-old *Usp26*$^{-/Y}$ mouse testes. Immunoblotting of MAD2, BUBR1, PLK1, and USP26 was performed in 2-month-old and 6-month-old *Usp26*$^{+/Y}$ and *Usp26*$^{-/Y}$ testes. H3Ser10p and Tub served as loading control.

F *Usp26*-deficient mice produced XY aneuploid round spermatids. FISH analysis of Chr X (green) and Chr Y (red) was performed in 2-month-old and 6-month-old *Usp26*$^{+/Y}$ and *Usp26*$^{-/Y}$ round spermatids. Nuclei were stained with DAPI (blue). The arrows indicate the Y chromosome, and the arrowheads indicate the X chromosome.

G Quantification of different types of round spermatids in 2-month-old *Usp26*$^{+/Y}$, *Usp26*$^{-/Y}$ mice (n = 3 independent experiments) and 6-month-old *Usp26*$^{+/Y}$ (n = 3 independent experiments), *Usp26*$^{-/Y}$ mice (n = 3 independent experiments). P = 0.0026 for XY spermatozoa in 6-month-old *Usp26*$^{+/Y}$ and *Usp26*$^{-/Y}$ mice. P = 0.0216 for O spermatozoa in 6-month-old *Usp26*$^{+/Y}$ and *Usp26*$^{-/Y}$ mice.

H *Usp26*-deficient mice produced XY aneuploid spermatozoa. FISH assay of Chr X (green) and Chr Y (red) was performed in 2-month-old and 6-month-old *Usp26*$^{+/Y}$ and *Usp26*$^{-/Y}$ spermatozoa. Nuclei were stained with DAPI (blue). The arrows indicate the Y chromosome, and the arrowheads indicate the X chromosome.

I Quantification of different types of spermatozoa in 2-month-old *Usp26*$^{+/Y}$, *Usp26*$^{-/Y}$ mice (n = 3 independent experiments) and 6-month-old *Usp26*$^{+/Y}$, *Usp26*$^{-/Y}$ mice (n = 5 independent experiments). P = 0.0195 for XY spermatozoa in 6-month-old *Usp26*$^{+/Y}$ and *Usp26*$^{-/Y}$ mice.

J *Usp26*-deficient mice could not produce Chr 8, Chr 10 aneuploid spermatozoa. FISH assay of Chr 8 (green) and Chr 10 (red) was performed in 6-month-old *Usp26*$^{+/Y}$ and *Usp26*$^{-/Y}$ spermatozoa. Nuclei were stained with DAPI (blue).

K Quantification of different types of spermatozoa in 6-month-old *Usp26*$^{+/Y}$, *Usp26*$^{-/Y}$ mice (n = 3 independent experiments). Data are presented as means ± SD.

L The disruption of *Usp26* produces XY aneuploid spermatozoa and results in the production of 41, XXY offspring.

Data information: In (C), (G), (I) and (K), data are presented as mean ± SD. **P < 0.01 (Student's t-test). Numerical source data for panels (C)/(G)/(I)/(K) can be found in Table EV5.
Source data are available online for this figure.

© 2021 The Authors

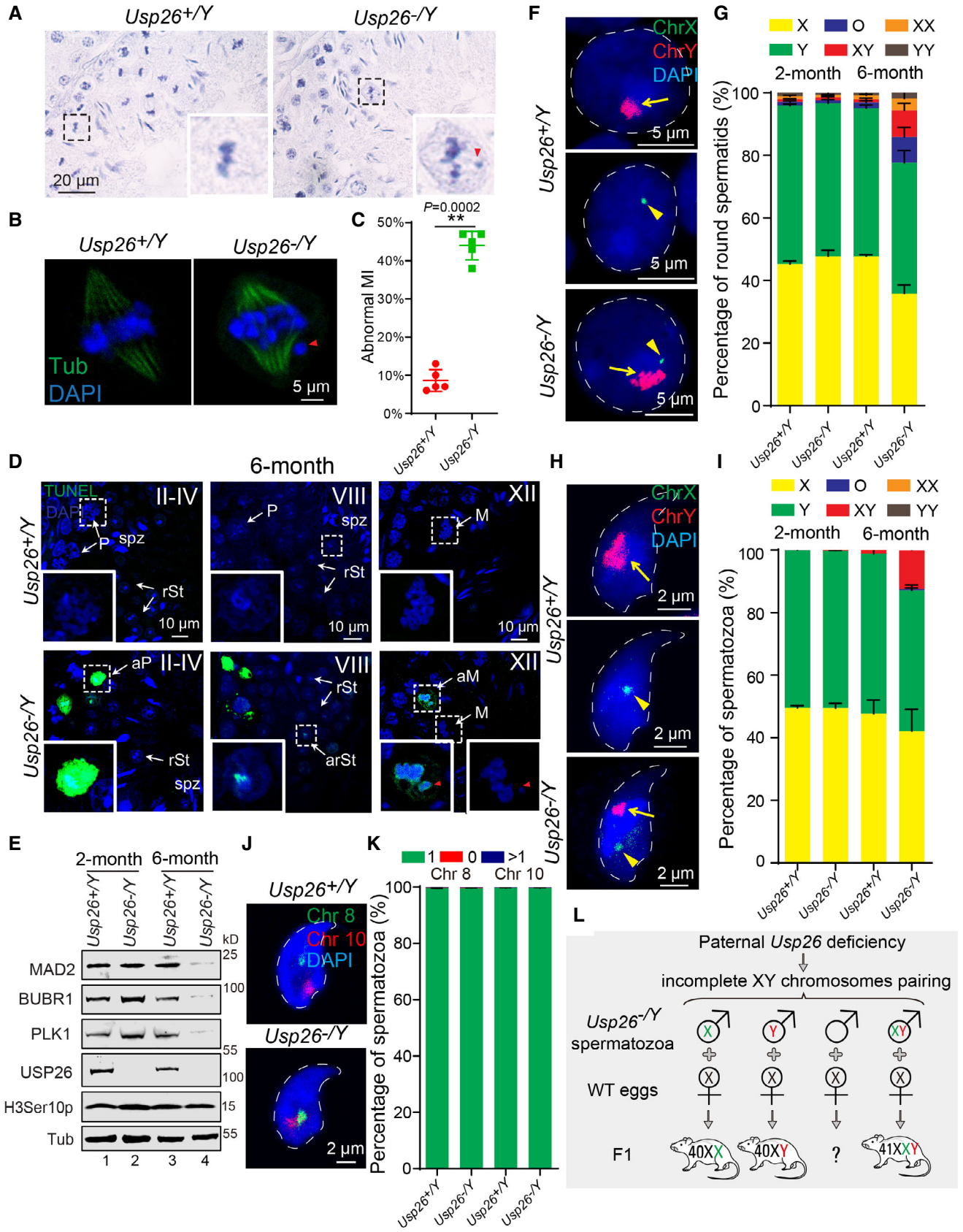

Figure 5.

© 2021 The Authors

were produced by 6-month-old *Usp26*$^{-/Y}$ mice compared with *Usp26*$^{+/Y}$ mice (Fig 5F and G). Therefore, spermatocytes with mis-segregated sex chromosomes that successfully escaped an apoptotic fate did indeed produce XY and O aneuploid round spermatids.

Beyond spermatogenesis, we also examined the XY and O aneuploid spermatozoa in *Usp26*$^{-/Y}$ mice. 6-month-old *Usp26*$^{-/Y}$ mice have a significantly higher proportion of XY aneuploid spermatozoa than *Usp26*$^{+/Y}$ mice (Fig 5H and I), while the proportions of chromosome 8 and 10 aneuploid spermatozoa in 6-month-old *Usp26*$^{-/Y}$ mice were quite low, similar to the control group (Fig 5J and K), indicating that disruption of *Usp26* apparently has little effect on autosome segregation during meiosis. We noted that 6-month-old *Usp26*$^{-/Y}$ mice produced only a very small number of O aneuploid spermatozoa (Fig 5H and I). As some round spermatids in 6-month-old *Usp26*$^{-/Y}$ mice were TUNEL positive (Fig 5D, middle panel), we speculate that O aneuploid round spermatids may be eliminated, thus preventing them from proceeding toward further spermatid differentiation. Collectively, these results indicate that disruption of *Usp26* apparently affects meiosis I, and support a model wherein the disruption of *Usp26* function perturbs sex chromosome pairing, causes their mis-segregation at metaphase I, and ultimately leads to XY aneuploid spermatozoa, which in turn results in the production of 41, XXY offspring (Fig 5L).

USP26 participates in sex chromosomes pairing by stabilizing TEX11

Previous studies have reported that the localization of USP26 is similar to that of TEX11, and *Tex11*-deficient spermatocytes have been shown to exhibit perturbed DSB repair and crossover formation (Adelman & Petrini, 2008; Yang *et al,* 2008). In our observations, we found that USP26 can co-localize with TEX11 at the XY body region (Fig EV4A–C). Given USP26's known function as a de-ubiquitinating enzyme that can regulate the stability of some proteins (Kit Leng Lui *et al,* 2017; Ning *et al,* 2017), we speculated that USP26 might stabilize TEX11 in the PAR region to regulate sex chromosomes pairing. To test this possibility, we examined potential interaction between USP26 and TEX11 by co-immunoprecipitation experiments with HEK293T cells, and found that these two proteins do indeed interact with each other (Fig 6A). We also found that USP26 could de-ubiquitinate TEX11 (Fig 6B). We measured the protein level of TEX11 in *Usp26*$^{-/Y}$ testes and found that TEX11 was dramatically reduced, supporting that USP26-mediated de-ubiquitination of TEX11 promotes TEX11 stability (Fig 6C).

Further, we generated a *Tex11*-knockout mice using the CRISPR-Cas9 system (Fig EV4D and E) that targeted exons 1–3 of the *Tex11* gene, referred to as *Tex11*$^{-/Y}$. We found unpaired sex chromosomes in *Tex11*$^{-/Y}$ spermatocytes (Fig 6D–G), which is consistent with previously reported results (Adelman & Petrini, 2008; Yang *et al,* 2008). When we carefully examined the seminiferous epithelium of *Tex11*$^{-/Y}$ mice, we found that although most of the spermatocytes arrested at the pachytene stage, spermatocytes in metaphase I and spermatozoa still existed in some seminiferous tubules in *Tex11*$^{-/Y}$ testis (Fig EV4F and G). As spindles with laggard chromosomes could also be observed in *Tex11*$^{-/Y}$ spermatocytes (Fig 6H and I), we speculated that separated sex chromosomes in *Tex11*$^{-/Y}$ spermatocytes might also lead to XY aneuploid spermatozoa. To test this possibility, we examined the X and Y chromosomes in *Tex11*$^{-/Y}$ spermatozoa and detected XY aneuploid spermatozoa in *Tex11*$^{-/Y}$ mice (Fig 6J), similar to our observations of the *Usp26*$^{-/Y}$ mice. Therefore, impairment of either *Tex11* or *Usp26* can disrupt sex chromosome pairing and can cause XY aneuploid sperm production. Given our finding that USP26-mediated de-ubiquitination can stabilize TEX11, USP26 might participate in sex chromosomes pairing by stabilizing TEX11.

The impact of *USP26* variants on XY aneuploid sperm production in humans

The studies in mice suggested that men with *USP26* variants should be fertile, but might be at a higher risk for producing XY aneuploid spermatozoa. We therefore measured the proportions of XY aneuploid spermatozoa in fertile men with four different *USP26* variants (Table EV4). Significantly higher proportions of XY aneuploid spermatozoa were found in the men harboring *USP26* variants compared with those without *USP26* variants (Fig 7A), clearly suggesting that these paternal *USP26* variations can raise the risk of producing KS offspring. Among these variations, the *USP26*-mutated haplotype

Figure 6. USP26 participates in sex chromosomes pairing by regulating the stability of TEX11.

A USP26 interacts with TEX11. *pRK-FLAG-Usp26* and *pEGFP-Tex11* were co-transfected into HEK293T cells. 24 h after transfection, cells were collected for immunoprecipitation (IP) with anti-FLAG antibody and analyzed with anti-FLAG and anti-GFP antibodies, respectively.

B USP26 modulates the ubiquitination of TEX11. *pRK-FLAG-Usp26*, *pEGFP-Tex11*, and *pCMV-HA-Ub* were transfected into HEK293T cells. At 24 h after transfection, cells were collected for immunoprecipitation (IP) with anti-GFP antibody and analyzed with anti-HA and anti-GFP antibodies, respectively.

C The TEX11 protein was greatly reduced in the *Usp26*$^{-/Y}$ testis. Immunoblotting of TEX11 was performed in 6-month-old *Usp26*$^{+/Y}$ and *Usp26*$^{-/Y}$ testes. Actin and SYCP3 served as the loading control.

D–F The X and Y chromosomes were unpaired in *Tex11*$^{-/Y}$ spermatocytes. Immunofluorescence analysis of SYCP3 (green), TRF1 (red), ATR (white) (D); SYCP3 (red), MLH1 (green), ATR (white) (E); Chr X-FISH (green), Chr Y-FISH (red) and SYCP3 (white) (F) was performed in in *Tex11*$^{+/Y}$ and *Tex11*$^{-/Y}$ spermatocytes. Nuclei were stained with DAPI (blue). The arrowheads indicate the X chromosome.

G Quantification of unpaired X and Y chromosomes in *Tex11*$^{+/Y}$ and *Tex11*$^{-/Y}$ mice (n = 4 independent experiments). Red dots indicate *Tex11*$^{+/Y}$ mice, and green dots indicate *Tex11*$^{-/Y}$ mice.

H Laggard chromosomes were observed in the metaphase I of *Tex11*$^{-/Y}$ spermatocytes. The arrowhead indicates the laggard chromosome.

I The proportion of metaphase I spermatocytes exhibiting laggard chromosomes in *Tex11*$^{+/Y}$ and *Tex11*$^{-/Y}$ mice spermatocytes (n = 3 independent experiments). Red dots indicate *Tex11*$^{+/Y}$ mice, and green dots indicate *Tex11*$^{-/Y}$ mice.

J *Tex11*-deficient mice produced XY aneuploid spermatozoa. FISH assay of Chr X (green) and Chr Y (red) was performed in *Tex11*$^{+/Y}$ and *Tex11*$^{-/Y}$ spermatozoa. Nuclei were stained with DAPI (blue). The arrows indicate the Y chromosome, and the arrowheads indicate the X chromosome.

Data information: In (G) and (I), data are presented as mean ± SD. $^{**}P < 0.01$ (Student's t-test). Numerical source data for panels (G)/(I) can be found in Table EV5. Source data are available online for this figure.

© 2021 The Authors

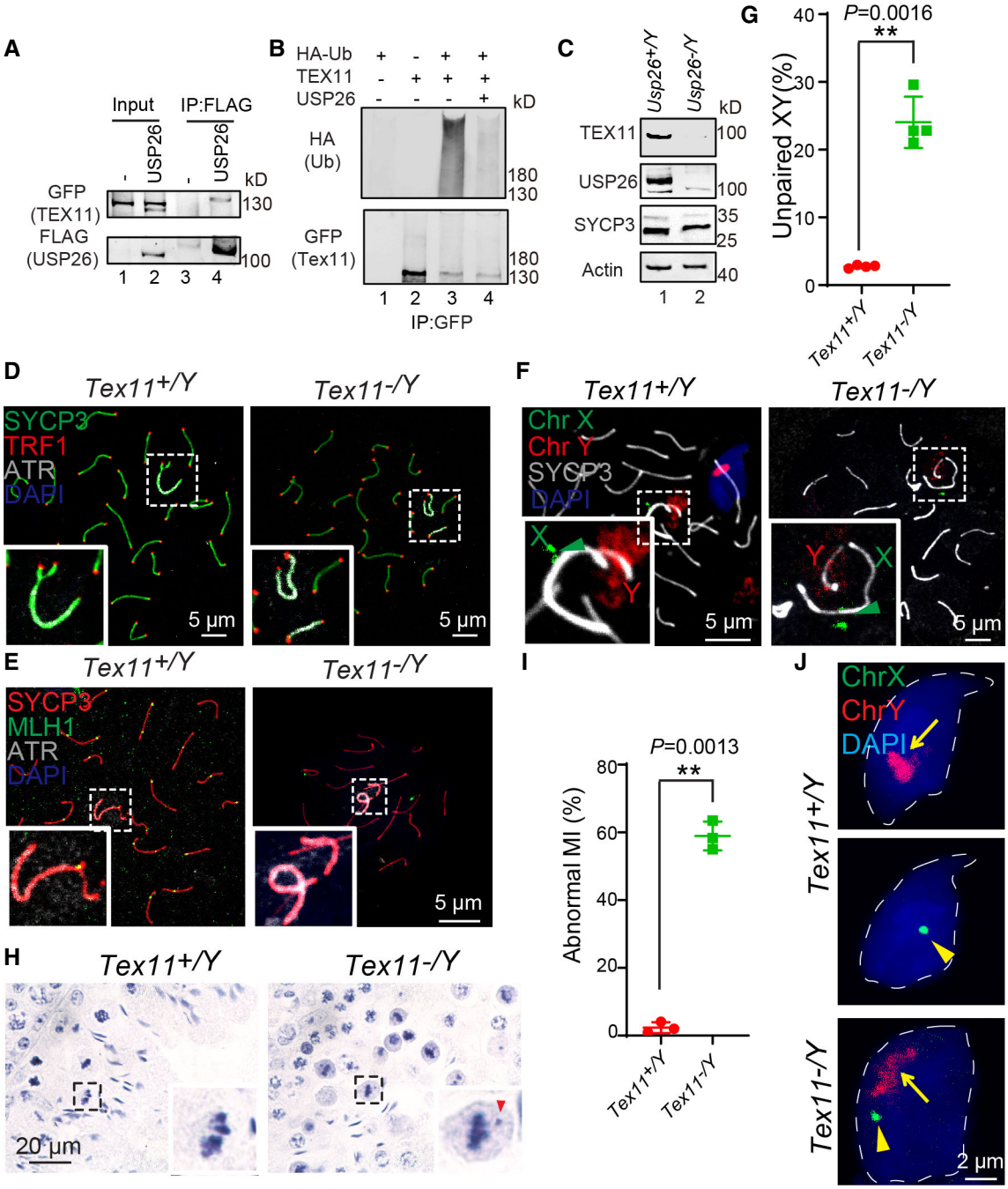

Figure 6.

(c.370–371insACA/494T>C/1423C>T) produced the highest proportion of XY aneuploid spermatozoa (Fig 7B and C). It was thus highly notable that this mutated haplotype was the most common among all of the KS patients from the 1st and 2nd cohorts (Table EV3).

We further investigated this mutated haplotype in 558 additional KS patients (Table EV1) and found 96 (17.20%) men who harbored it; thus, a total of 155 men in our total cohort of 1,020 KS patients (15.20%) had this mutated haplotype. Therefore, the frequency of *USP26* variants in our KS cohort ranged from 13.84 to 26.85%. Because the extra X chromosome in KS is equally likely to be of maternal or paternal origin (Hassold & Hunt, 2001; Thomas & Hassold, 2003), paternal-origin KS cases associated with *USP26* variants would be able 6.93–13.43%. To test this, we collected a total of 62 core KS family samples and found that 45 KS patients were of maternal origin, while 17 KS patients were of paternal origin. Among the paternal-origin KS families, we identified two families (11.76% [2/17]) in which the father of the KS patient harbored the *USP26*-mutated haplotype (Fig 7D). Sanger sequencing showed the father of the KS patient (I-1) had the *USP26*-mutated haplotype (c.370_371insACA/494T>C/1423C>T), while the mother of the KS

 © 2021 The Authors

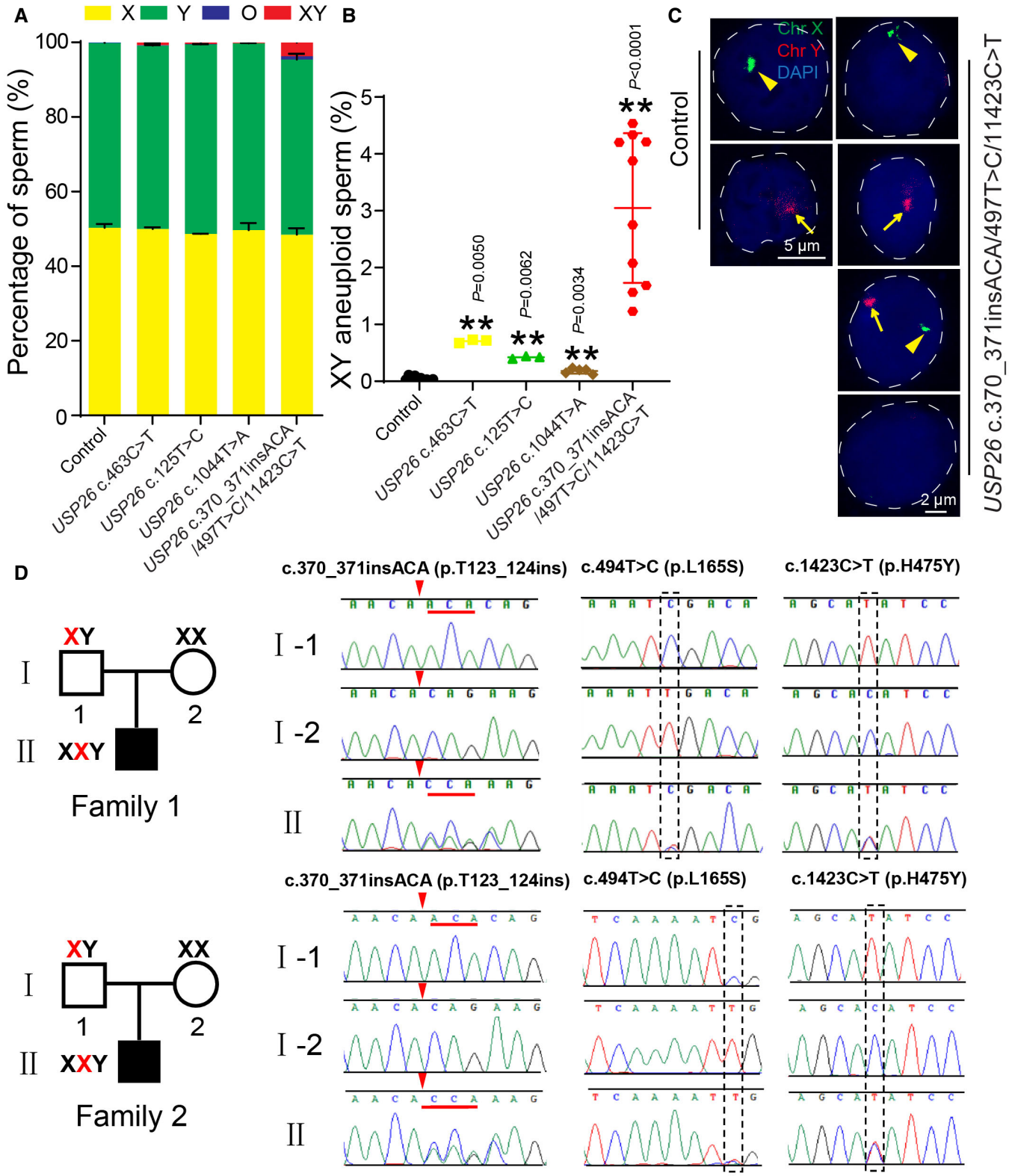
A
X
Y
O
XY
Percentage of sperm (%)
100
80
60
40
20
0
Control
USP26 c.463C>T
USP26 c.125T>C
USP26 c.1044T>A
USP26 c.370_371insACA /497T>C/11423C>T
B
XY aneuploid sperm (%)
5
4
3
2
1
0
P=0.0050
P=0.0062
P=0.0034
P<0.0001
**
C
Control
Chr X
Chr Y
DAPI
5 μm
2 μm
USP26 c.370_371insACA/497T>C/11423C>T
D
c.370_371insACA (p.T123_124ins)
c.494T>C (p.L165S)
c.1423C>T (p.H475Y)
XY
XX
XXY
I
II
1
2
I -1
I -2
Family 1
Family 2

Figure 7.

Figure 7. Fertile men with *USP26* mutations produce XY aneuploid spermatozoa.

A, B Quantification of different types of spermatozoa in fertile men with or without *USP26* mutations. The spermatozoa from fertile men without *USP26* mutations (n = 10 independent experiments); fertile men contained the *USP26* c.463C>T mutation (The sample was analyzed in three repeated experiments), the *USP26* c.125T>C mutation (n = 2 independent experiments, one sample was analyzed in two repeated experiments), the *USP26* c.1044T>A mutation (n = 5 independent experiments), and the *USP26* c.370_371insACA/494T>C/1423C>T mutation (n = 10 independent experiments) were collected to perform Chr X and Chr Y-FISH. *P*-values are shown for comparison to fertile men without *USP26* mutations.

C The fertile men with the *USP26*-mutated haplotype produced XY and O aneuploid spermatozoa. FISH assay of Chr X (green) and Chr Y (red) was performed in fertile men with or without the *USP26*-mutated haplotype. Nuclei were stained with DAPI (blue). The arrows indicate the Y chromosome, and the arrowheads indicate the X chromosome.

D Squares denote male family members, circles denote female family member; a solid symbol indicates affected KS member, open symbols represent unaffected KS family members. The X labeled with red color indicates the X chromosome with the *USP26*-mutated haplotype (c.370_371insACA/494T>C/1423C>T). All family members were Sanger sequenced.

Data information: In (A) and (B), data are presented as mean ± SD. $^{**}P < 0.01$ (Student's *t*-test). Numerical source data for panels (A)/(B) can be found in Table EV5.

patient (I-2) had no mutations in the coding region of *USP26* (Fig 7D). The KS patient (II) had the classical 47, XXY karyotype and had the heterozygous *USP26*-mutated haplotype (Fig 7D). Further short tandem repeat (STR) polymorphic linkage analysis also confirmed that the extra X chromosome in the KS patient came from his father (Figs 7D and EV5A). Thus, these results further support that paternal *USP26* mutation can result in KS offspring.

Given our observation that, with increasing age, paternal $Usp26^{-/Y}$ in mice results in oligospermia and produces KS offspring, we speculated that humans with *USP26* variants might display age-dependent oligospermia and/or elevated rates of KS offspring. As the mutated haplotype (c.370–371insACA/494T>C/1423C>T) of *USP26* was the most common *USP26* variants in the KS patients (Table EV3), we selected this mutated haplotype and further investigated them in 195 oligoasthenozoospermia patients. We found that 10.26% (20/195) of these oligospermia patients contained such *USP26* cluster mutations (Fig EV5B). Moreover, we found that the population of oligospermia patients harboring the *USP26* cluster mutations were significantly older than fertile men with the same mutation (Fig EV5B). Therefore, consistent with our findings from experiments with 2- and 6-month-old $Usp26^{-/Y}$ male mice, *USP26* mutations in humans might be associated with oligospermia in an age-dependent manner.

Discussion

Although impaired pairing between XY chromosomes has been speculated to be a major cause of paternal-origin KS (Hassold *et al,* 1991; Thomas *et al,* 2000), few studies have tried to address this hypothesis before. The X and Y chromosomes in males only have a small region of homology for pairing, which is known as the PAR (Raudsepp *et al,* 2012), and it is now understood that XY chromosome pairing in this region is apparently exclusively mediated by DSB formation and subsequent meiotic recombination (Kauppi *et al,* 2011). Compared to autosomes, the production of DSBs and subsequent homologous pairing and synapsis of sex chromosomes occurs substantially slower and also requires special meiotic DSB machinery and meiotic recombination components that have been shown to appear as so-called XY bodies in the pachytene and diplotene stages of meiosis (Kauppi *et al,* 2011; Lu *et al,* 2013). This foundational information about impaired recombination between paternal sex chromosomes in the PAR during meiosis I has informed much speculation about the etiology of paternal-origin KS (Hassold *et al,* 1991; Thomas *et al,* 2000).

We found that *USP26* variations might be responsible for promoting paternal-origin KS, and observed both that the USP26 protein is localized on the XY body region and that its genetic disruption results in unpaired sex chromosomes (Fig 4B–F). USP26 interacts with TEX11 and regulates the stability of TEX11 via de-ubiquitination (Fig 6A–C). As TEX11 has been found to interact with SYCP2, NBS1, and SHOC1, and to promote synapsis and crossover formation (Adelman & Petrini, 2008; Yang *et al,* 2008; Guiraldelli *et al,* 2018), USP26's modulation of TEX11 stability may regulate sex chromosome recombination and pairing. Although the disruption of TEX11 has been confirmed to cause male infertility in both mice and humans, at least one reported *Tex11* hypomorphic mouse model is still fertile (Adelman & Petrini, 2008; Yang *et al,* 2008; Yatsenko *et al,* 2015). Given that disrupted *Tex11* affects sex chromosomes pairing (Fig 6D–G) (Adelman & Petrini, 2008; Yang *et al,* 2008), it is reasonable to speculate that some *TEX11* mutations might also increase the rate of KS offspring production.

Errors in meiotic recombination and chromosome synapsis have been shown to increase the probability that cells will progress to metaphase with univalent chromosomes (Tempest, 2011). In theory, if the sex chromosomes randomly segregated at meiosis I, the spermatozoa would have 25% distributions of X, Y, XY, and O spermatozoa. If the sex chromosomes randomly segregated at meiosis II, there would be 25% distributions for X, Y, and O spermatozoa, as well as 12.5% each for XX and YY. We found that there were around 10% XY, but no XX or YY spermatozoa produced from 6-month-old $Usp26^{-/Y}$ male mice (Fig 5H and I). Importantly, 6-month-old $Usp26^{-/Y}$ male mice sired XXY mice (Fig 2G). These results indicate that once *Usp26* is knocked out, sex chromosomes cannot efficiently pair and synapse, which in turn results in sex chromosomes randomly segregating during meiosis I, producing XY aneuploid spermatozoa, and ultimately leading to the production of XXY mice (Fig 5L). Given our observation that around 9% XY and O aneuploid round spermatids were detected in 6-month-old $Usp26^{-/Y}$ male mice (Fig 5F and G), and considering that some round spermatids in 6-month-old $Usp26^{-/Y}$ mice were TUNEL positive (Fig 5D), we speculate that the O aneuploid round spermatids may die at this stage, thereby preventing them from proceeding further in the spermatid differentiation process. Thus, disruption of *Usp26* is apparently deleterious for the survival of aneuploid O

 © 2021 The Authors

round spermatids, helping explain the absence of O aneuploid spermatozoa in the *Usp26*$^{-/Y}$ mice.

Recent studies have also examined the functional role of USP26 in mouse spermatogenesis (Felipe-Medina *et al,* 2019; Sakai *et al,* 2019; Tian *et al,* 2019), although these studies did not report the production of 41, XXY offspring. One study only examined 2-month-old *Usp26*$^{-/Y}$ male mice (Felipe-Medina *et al,* 2019), and although the authors of the other study observed a subfertility phenomenon in elder *Usp26*$^{-/Y}$ mice (Tian *et al,* 2019), they did not examine sex chromosome pairing in aged *Usp26*$^{-/Y}$ male mice, and they did not genotype the offspring. It is worth considering that the very low rate of 41, XXY offspring sired by *Usp26*$^{-/Y}$ male mice makes it very easy to overlook this phenomenon. As it has been reported that the *Tex11* exon 3 deletion mouse was fertile (Adelman & Petrini, 2008), it would be informative to genotype a large number of progeny from other *Usp26*$^{-/Y}$ male mouse models. In addition to TEX11, USP26 has also been reported interact with androgen receptor (AR) and modulate its ubiquitination and stability (Dirac & Bernards, 2010; Tian *et al,* 2019; Wang *et al,* 2020), indicating that USP26 might play multiple functional roles in spermatogenesis.

In addition to fertility, we noted that the proportion of 41, XXY offspring was also associated with the age of *Usp26*$^{-/Y}$ male mice, and 41, XXY offspring were produced by 6-month-old but not by 2-month-old *Usp26*$^{-/Y}$ mice (Fig 2G). Because a number of *Usp26*$^{-/Y}$ spindles exhibiting laggard chromosomes were observed (Fig 5A–C), and given that some of the cells with these chromosomes were TUNEL negative (Fig 5D), it is reasonable to speculate that the SAC may be inactive in aged *Usp26*$^{-/Y}$ mice. Indeed, we found that the testes of 6-month-old *Usp26*$^{-/Y}$ male mice had reduced levels of three known SAC-related proteins (Fig 5E). Previous studies found that reduced levels of the SAC protein MAD2 in *Spo11β*-only^{mb} male mice, which also show unpaired sex chromosomes, attenuate the apoptotic response to mis-segregating sex chromosomes and cause the formation of XY aneuploid spermatozoa in mice (Faisal & Kauppi, 2017). Therefore, the inactive spindle assembly checkpoint in aged *Usp26*$^{-/Y}$ male mice may lead to the production of aneuploid spermatozoa, which could further exacerbate declines in fertility.

Reports have associated *USP26* with nonobstructive azoospermia, but other studies have presented contradictory results, so this association remains debatable (Xia *et al,* 2014; Zhang *et al,* 2015; Luddi *et al,* 2016; Ma *et al,* 2016). Both our and other reports (Felipe-Medina *et al,* 2019; Tian *et al,* 2019) have demonstrated that 2-month-old *Usp26*$^{-/Y}$ male mice were fertile, but with increasing age, both the pregnancy rate and litter size were reduced (Fig 2C and D) (Tian *et al,* 2019), suggesting that the fertility of *Usp26*$^{-/Y}$ male mice is highly related to age. Furthermore, we found that the population of oligospermia patients harboring the *USP26* cluster mutations were older than fertile men with the same mutation (Fig EV5B). Therefore, it is possible that young men with *USP26* mutations might be fertile but might lose their fertility as they get older, and it is plausible to expect later diagnosis with oligospermia and eventually azoospermia. These findings about the age-related phenotypes in spermatogenesis are potentially relevant for genetic counseling relating to KS, and perhaps individuals with *Usp26* mutations could be counseled to undertake cryopreservation of sperm at younger ages.

In addition to mutations in *USP26*, we show that XY aneuploid spermatozoa are present in *Tex11*$^{-/Y}$ mice (Fig 6J), and we also found a *TEX11* variant (c.A344G[p.K115R] and c.G1306A[p.E436K]) in our 1st KS cohort (Table EV1), suggesting that *TEX11* mutations may also be responsible for the paternal origin of KS. Recently, 47 different *TEX11* mutations have been identified, including 25 in azoospermic patients and 22 in fertile men (Yang *et al,* 2015; Yatsenko *et al,* 2015; Sha *et al,* 2018). It thus appears that distinct *TEX11* variants confer discrete consequences, for example, leading to completely male infertile phenotypes or to fertile phenotypes accompanied by KS production. It bears emphasizing that only ~ 20% of the KS cases detected in our cohort can be attributed to mutations in either *USP26* or *TEX11*, so it is clear that we have only encountered the tip of the KS genetic iceberg. More efforts are definitely needed to help shed light on the molecular basis of KS production.

Non-disjunction of sex chromosomes during meiosis may also lead to other types of sex chromosome aneuploidies such as Turner syndrome (XO), trisomy X (XXX), and XYY (Skuse *et al,* 2018). This kind of Mendelian inheritance we delineated for KS should thus be considered in other studies of sex chromosome aneuploidy disorders. As the random segregation of sex chromosomes at meiosis I and meiosis II may produce different types of aneuploid spermatozoa, the genetic etiology for these sex chromosome aneuploidies may be different. Future studies should pay attention to those individuals who are fully fertile but who harbor mutations that may increase the production of other types of sex chromosome aneuploidy. The etiology of these sex chromosome aneuploidies needs further investigation, and such sex chromosome disorder-related mutations could be incorporated into clinical genetic counseling to notify couples harboring these mutations that they may have high risk for producing offspring with sex chromosome aneuploidy.

Materials and Methods

Study participants

The study cohort was composed of 1,020 KS patients (range 22–28 years old; Table EV1) from the Center for Reproductive Medicine, Shandong University, Jinan, China. The diagnosis in infertile men with KS was confirmed at least twice by means of semen analysis according to the guidelines of the World Health Organization (World Health Organization, 2001) and the peripheral blood cytogenetic karyotype 47,XXY (Seo *et al*, 2004). The chimeric type of KS was not included in this study. The diagnosis in oligoasthenozoospermia patients was confirmed by semen analysis according to the guidelines of the World Health Organization (World Health Organization, 2001). A total of 272 DNA samples of unrelated, anonymous, native male donors were used as controls. The study protocol was approved by the Institutional Review Board (IRB) of the Center for Reproductive Medicine of Shandong University ([2017] Ethical Review#31). Before participation, all the candidates provided written, informed consent.

Genetic analysis

Genomic DNA was extracted from peripheral blood leukocytes. Whole-exome sequencing was performed in 108 unrelated KS patients to identify causative mutations. Sure Select Human All Exon V5 kits (Agilent Technologies, 5190-6208) were used for whole-exome capture and enrichment, according to the product

© 2021 The Authors

instructions. Exome sequencing was performed on the HiSeq X10 sequencing platform (Illumina). Burrows-Wheeler Alignment software was used for aligning sequence reads to the human reference sequence (UCSC Genome Browser hg19). Sequence variants including single nucleotide polymorphisms and insertion/deletions were annotated with ANNOVAR software. The variants were divided into the following four subtypes according to their frequencies, genomic localization, and potential deleterious effects: high (exonic region, allele frequencies ≤ 0.01 in both the ExAC Browser and 1000 Genomes Project, and predicted to be potentially deleterious), likely high (exonic or splicing region, allele frequencies ≤ 0.01 in the ExAC Browser or 1000 Genomes Project, and predicted to be potentially deleterious), medium (exonic or splicing region, allele frequencies ≤ 0.01 in ExAC Browser or 1000 Genomes Project), and low.

The generation of *Usp26* and *Tex11* knockout mice

The *Usp26*-deletion mice (16bp-, 163bp-deletion) were generated by Laboratory Animal Center, IOZ, CAS (Beijing, China), the *Usp26* 2664bp-deletion mice and *Tex11* deletion mice were generated by Cyagen Biosciences Inc (Guangzhou, China). The T7 promoter and guiding sequences were added to the sgRNA by PCR amplification using the following primers: *Usp26*-ugRNA1: AGT CCA GAT GTG GAG TGC AAA GG; *Usp26*-ugRNA2: TAA ATG CTC AAG TCC AGA TGT GG; *Usp26*-dgRNA3: GTA ATT CTG GTC TTC GCC ATA GG; *Usp26*-dgRNA4: GGT CTT CGC CAT AGG TTT GAA GG; and *Usp26*-dgRNA5: GTT GTC TCC TTA GGT AAA CTT GG; *Usp26*-dgRNA6: GAA GGA CAG ATA ATT AGC CCA GG; *Tex11*-ugRNA3: TCC GAT AGG TAT GTC CAC TGG GG; *Tex11*-ugRNA4: GGA CCT AAG TAC AGC TCA AGG GG. B6D2F1 (C57BL/6 × DBA2, RRID: IMSR_JAX:100006) female mice and ICR female mice were used as embryo donors and foster mothers, respectively. Superovulated female B6D2F1 mice (6–8 weeks old) were mated with B6D2F1 stud males, and the fertilized embryos were collected from the oviducts. Cas9 mRNA (20 ng) and sgRNA (10ng) were injected into the cytoplasm of fertilized eggs with well-recognized pronuclei in M2 medium (Sigma, M7167-50ml, Santa Clara, CA). The injected zygotes were cultured in KSOM (modified simplex-optimized medium, Millipore) with amino acids at 37°C under 5% CO_2 in air, and 15–25 blastocysts were transferred into the uterus of pseudopregnant ICR females. We obtained one type of *Tex11*-deletion mouse and three types of *Usp26*-deletion mice, including a 16 bp deletion in the *Usp26* coding region, a 163bp deletion in the *Usp26* coding region, and a 2664bp deletion in the *Usp26* coding region. To generate semi-cloned embryos, DKO-AG-haESCs with *Usp26*-N-HA were arrested in M-phase and then used for intracytoplasmic injection as described previously (Zhong *et al*, 2015). Intracytoplasmic AG-haESC injection (ICAHCI) embryos were cultured in KSOM medium for 24 h to reach the two-cell stage. A total of 15–20 two-cell embryos were transferred into each oviduct of pseudopregnant ICR females at 0.5 days post-coitus (dpc). *Usp26*-N-HA semi-cloned mice (F0) were crossed with WT C57BL/6J male mice to generate heterozygous *Usp26*-N-HA F1 male mice for our experiments. All of the animal experiments were performed according to approved institutional animal care and use committee (IACUC) protocols (#08–133) of the Institute of Zoology, Chinese Academy of Sciences.

Antibodies

Mouse antibodies to γH2AX (05-636), ATMps1981 (05-740), UbH2A (05-678), and Pol II (05-952) were purchased from Merck Millipore (Darmstadt, Germany). Rabbit antibodies to USP26 (A7999), TEX11 (A15868), MAD2 (A11469), BUBR1 (A14525), and α-Tubulin (AC007) were purchased from ABclonal (Wuhan, China). Rabbit antibody to phospho-Histone H3 (Ser10) was purchased from Cell Signaling Technology (Danvers, USA). Mouse antibodies to MLH1 (51-1327GR) were purchased from BD Pharmingen (San Diego, USA). Mouse anti-TRF1 (ab10579) anti-HA (ab130275), rabbit antibodies against SYCP3 (150292), and PLK1 (ab189139) were purchased from Abcam (Cambridge, USA). Sheep antibody to MDC1 was purchased from Bio-Rad (Hercules, USA). Rabbit antibodies to SYCP1 (NB300-228c) and MRE11 (NB100-142) were purchased from Novus Biologicals (Littleton, USA). Mouse antibodies to SYCP3 (SC-74569), goat antibodies to ATR (SC-1187), goat antibody to BRCA1 (SC-1553), and rabbit antibodies to DMC1 (SC-22768) were purchased from Santa Cruz Biotechnology (Dallas, USA). Anti-Histone 3 (17168-1-AP) was purchased from ProteinTech Group (Rosemont, USA). Anti-α-Tubulin−FITC antibody (F2168) was purchased from Sigma-Aldrich (St. Louis, USA). Anti-FLAG (M20008), anti-HA (M20003), anti-GFP (M20004), and anti-Pan-Actin (M20010L) were purchased from Abmart (Shanghai, China). USP26 polyclonal antibody for immunoblotting was generated in rabbits using the corresponding recombinant proteins as antigens. Goat anti-rabbit FITC (ZF-0311), goat anti-mouse FITC (ZF-0312), and goat anti-mouse TRITC (ZF-0313)-conjugated secondary antibodies were purchased from Zhong Shan Jin Qiao (Beijing, China). Alexa Fluor 680-conjugated goat anti-mouse (A21057) and Alexa Fluor 680-conjugated goat anti-rabbit (A21109) antibodies for immunoblotting were purchased from Invitrogen (Carlsbad, USA).

Assessment of the fertility of *Usp26*-deficient mice

The fertility assessment experiments were performed as previously described (Zhu *et al*, 2018). Each male mouse (8 or 9 weeks of age) was caged with two wild-type ICR females (7 or 8 weeks of age), and their vaginal plugs were checked every morning. The plugged females were separated and caged individually, and the pregnancy outcomes were recorded. If a female did not generate any pups by 22 dpc, the mouse was deemed not pregnant and was euthanized to confirm that result. Each male underwent 6–10 cycles of the above breeding assay.

Epididymal sperm count

The caudal epididymis was dissected. Spermatozoa were squeezed out from the caudal epididymis and incubated for 30 min at 37°C under 5% CO_2. The incubated sperm medium was then diluted 1:500 and transferred to a hemocytometer for counting.

Tissue collection and histological analysis

Testes from at least three mice for each genotype were dissected immediately after euthanasia, fixed in 4% (mass/vol) paraformaldehyde (PFA; Solarbio, Beijing, China, P1110) for up to 24 h, stored in 70% (vol/vol) ethanol, embedded in paraffin, and cut into 5 μm sections and mounted on glass slides. After deparaffinization, the slides were stained with hematoxylin and eosin for histological analysis. For PAS staining, testes were fixed with Bouin's fixatives (Polysciences, Warrington, PA). After deparaffinization, the slides were

 © 2021 The Authors

stained with PAS and hematoxylin. The stages of seminiferous epithelium cycle and spermatid development were determined as previously described (Hess & Renato de Franca, 2008).

Immunofluorescence

The spermatocytes were spread on glass slides for immunostaining. After air drying, the slides were washed with PBS three times and blocked with 5% bovine serum albumin (Amresco, Solon, OH, AP0027). The primary antibody was added to the sections and incubated at 4°C overnight, followed by incubation with the secondary antibody. The nuclei were stained with 4′,6-diamidino-2-phenylindole (DAPI). The immunofluorescence images were taken immediately using an LSM 780/710 microscope (Zeiss, Germany) or SP8 microscope (Leica, Germany).

Immunoprecipitation

pRK-FLAG-Usp26 and *pEGFP-Tex11* were co-transfected into HEK293T cells. Transfected cells were lysed in TAP lysis buffer (50 mM HEPES-KOH, pH7.5, 100 mM KCl, 2 mM EDTA, 10% glycerol, 0.1% NP-40 10 mM NaF, 0.25 mM Na_3VO_4, 50 mM β-glycerol phosphate) plus protease inhibitors (Roche, 04693132001) for 30 min on ice and centrifuged at 13,000 *g* for 15 min. For immunoprecipitation, cell lysates were incubated with anti-FLAG antibody overnight at 4°C and then incubated with protein A-Sepharose (GE, 17-1279-03) for 2 h at 4°C. Thereafter, the precipitants were washed two times with IP buffer (20 mM Tris, pH 7.4, 2 mM EGTA, 1% NP-40), and the immune complexes were eluted with sample buffer containing 1% SDS for 10 min at 55°C and analyzed by immunoblotting.

Human sperm preparation and sperm FISH analysis

Collected seminal fluid was first washed three times in PBS with 6 mM EDTA to eliminate any impurities (by centrifuging at 300 *g* for 5 min), fixed with Carnoy's solution (3:1 absolute methanol: glacial acetic acid) twice, and spread on a slide prior to sperm FISH. The sperm heads were decondensed with 1N NaOH and dehydrated through an ethanol series (70, 85, 100%). Slides were placed on a 42°C warmer to evaporate the remaining ethanol and then hybridized with probe (CEP Chromosome Enumeration DNA FISH Probe, 466279) for at least 16 h in a prewarmed humidified box. The slices were washed sequentially in 2 × saline sodium citrate (SSC) with 0.1% Tween (twice) at 65°C and with 2 × SSC (twice) at room temperature for 5 min each time, then stained with DAPI. The sperm were scored under an SP8 microscope (Leica, Germany) with a 63× objective to digitize the image, and records of every sperm with an abnormal number of hybridization domains were taken by digitizing the microscopic image. As men with *USP26* variants, c.125T>C and c.463C>T were less than three, these samples were analyzed in three repeated experiments.

Mouse sperm preparation and sperm FISH analysis

The cauda epididymis was isolated from $Usp26^{+/Y}$ and $Usp26^{-/Y}$ mice, and sperm were released from the cauda epididymis and incubated at 37°C for 30 min under 5% CO_2. Collected sperm were first washed with PBS to eliminate any impurities (by centrifuging at 300 *g* for 5 min), fixed with Carnoy's solution twice, and spread on a slide prior to sperm FISH. The sperm heads were decondensed with 1N NaOH and incubated for a maximum of 10 min in 5 mM DTT at 37°C, then dehydrated through an ethanol series (70, 85, 100%). Slides were placed on an 80°C warmer to evaporate the remaining ethanol. After denaturation at 85°C for 10 min with the probe (Empire Genome, Chromosome X Green [MCENY-10-GR], Chromosome Y Red [MCENY-10-RE]; MetaSystems, Chromosome 8 Green [D-1408-050-FI], Chromosome 10 orange [D-1410-050-OR]), they were hybridized for 24 h at 37°C in a prewarmed humidified box. The slices were washed sequentially in 2 × SSC with 0.1% Tween (twice) at 65°C and with 2 × SSC (twice) at room temperature for 5 min each time, then stained with DAPI.

Short tandem repeat polymorphic linkage analysis

The STR markers selected in the present study were DYSII, STR44, and STR45. The DYSII primers were DYSII-F: CAT CCA AAT TAA GCA ACC AAC A; DYSII-R: CAG GCA TCA TTC AGA TTG GA. STR44 primers were STR44-F: TGC TTA TTG CCC TGA CAA TTT; STR44-R: TTC CTT GAG GAA TGG GAG TC. STR45 primers were STR45-F: CAG CCT TCA GGA GAC TTG CT; STR45-R: CCT GTG ACC TTC CCA CTC AT. PCR was conducted in a total volume of 20 μl containing 2 μl genomic DNA, 1 μl primer pair mix, 1.6 μl dNTPs and 2 μl 10 × PCR Buffer 0.1 μl Taq polymerase, and 13.3 μl ddH_2O. After 3 min of denaturation at 94°C, 35 cycles of the following were performed: denaturation at 94°C for 30 s, annealing at 58°C for 30 s, extension at 72°C for 30 s, and final extension at 72°C for 5 min. Each of the PCR products was mixed with 9 μl standards. Following denaturation at 95°C for 5 min and rapid cooling on ice, the mixture was electrophoresed and separated by capillary electrophoresis on an ABI 3500 Genetic Analyzer.

Statistical analysis

All data are presented as the mean ± SD. The statistical significance of the differences between the mean values for the different genotypes was measured by Student's *t*-tests with two-tailed distribution. The data were considered significant when the *P*-value was less than 0.05 (*) or 0.01 (**).

Data availability

The KS patient exome series data are available at the Genome Sequence Archive in National Genomics Data Center, China National Center for Bioinformation/Beijing Institute of Genomics, Chinese Academy of Sciences, BioProject: PRJCA004739, reference number HRA000736 (https://bigd.big.ac.cn/gsa-human/browse/HRA000736). Exome data for individual patients cannot be made publicly available for reasons of patient confidentiality. Qualified researchers may apply for access to these data, pending institutional review board approval.

Expanded View for this article is available online.

Acknowledgements
In addition to the authors, S. Lu, X. Li, T. Zhang, M. Gao, Y. Cao, L. Cheng, Z. Wang, and Y. Ning of the Center for Reproductive Medicine, Cheeloo College of

© 2021 The Authors

Medicine, and Key laboratory of Reproductive Endocrinology of Ministry of Education, Shandong University participated in data collection and site monitoring. This work was supported by the National Key R&D Program of China (2016YFA0500901), the National Science Fund for Distinguished Young Scholars (81925015), the Strategic Priority Research Program of the Chinese Academy of Sciences (XDA16020700), the National Natural Science Foundation of China (31771501, 82071699, 81771538, 81571497, 31771588, 91649202), the Youth Innovation Promotion Association CAS (2018109), and the Fundamental Research Funds of Shandong University. *Usp26-HA* mice were supplied by Genome Tagging Project (GTP) Center, CEMCS, CAS, which was supported by Shanghai Municipal Commission for Science and Technology Grants (19411951800).

Author contributions

Z-JC and WL designed the experiments and wrote the article. CL, HL, HZ, and LW performed most of the experiments and assisted in drafting the manuscript. ML, FC, RZ, SY, WWL, LYW, XS, SS, and HG enrolled participants. XW, LW, and YL did the statistical analyses. JJ and JL generated the *Usp26-HA* mouse model. Z-JC, WL, HL, QC, FG, and ML supervised the project. Z-JC had a primary responsibility for final content. All authors were involved in data collection, interpreted the data, provided critical input to the manuscript, and approved the final manuscript.

Conflict of interest

The authors declare that they have no conflict of interest.

References

Acquaviva L, Boekhout M, Karasu ME, Brick K, Pratto F, Li T, van Overbeek M, Kauppi L, Camerini-Otero RD, Jasin M *et al* (2020) Ensuring meiotic DNA break formation in the mouse pseudoautosomal region. *Nature* 582: 426 – 431

Adelman CA, Petrini JH (2008) ZIP4H (TEX11) deficiency in the mouse impairs meiotic double strand break repair and the regulation of crossing over. *Plos Genet* 4: e1000042

Arafat M, Zeadna A, Levitas E, Vardi IH, Samueli B, Shaco-Levy R, Dabsan S, Lunenfeld E, Huleihel M, Parvari R (2020) Novel mutation in USP26 associated with azoospermia in a Sertoli cell-only syndrome patient. *Mol Genet Genom Med* 8: e1258

Baker SM, Plug AW, Prolla TA, Bronner CE, Harris AC, Yao X, Christie DM, Monell C, Arnheim N, Bradley A *et al* (1996) Involvement of mouse Mlh1 in DNA mismatch repair and meiotic crossing over. *Nat Genet* 13: 336 – 342

Barchi M, Roig I, Di Giacomo M, de Rooij DG, Keeney S, Jasin M (2008) ATM promotes the obligate XY crossover and both crossover control and chromosome axis integrity on autosomes. *PLoS Genet* 4: e1000076

Bonomi M, Rochira V, Pasquali D, Balercia G, Jannini EA, Ferlin A; Klinefelter ItaliaN Group (KING) (2017) Klinefelter syndrome (KS): genetics, clinical phenotype and hypogonadism. *J Endocrinol Invest* 40: 123 – 134

Cherry SM, Adelman CA, Theunissen JW, Hassold TJ, Hunt PA, Petrini JH (2007) The Mre11 complex influences DNA repair, synapsis, and crossing over in murine meiosis. *Curr Biol* 17: 373 – 378

Corona G, Pizzocaro A, Lanfranco F, Garolla A, Pelliccione F, Vignozzi L, Ferlin A, Foresta C, Jannini EA, Maggi M *et al* (2017) Sperm recovery and ICSI outcomes in Klinefelter syndrome: a systematic review and meta-analysis. *Hum Reprod Update* 23: 265 – 275

Dirac AMG, Bernards R (2010) The deubiquitinating enzyme USP26 is a regulator of androgen receptor signaling. *Mol Cancer Res* 8: 844 – 854

Eskenazi B, Wyrobek AJ, Kidd SA, Lowe X, Moore D, Weisinger K, Aylstock M (2002) Sperm aneuploidy in fathers of children with paternally and maternally inherited Klinefelter syndrome. *Hum Reprod* 17: 576 – 583

Faisal I, Kauppi L (2017) Reduced MAD2 levels dampen the apoptotic response to non-exchange sex chromosomes and lead to sperm aneuploidy. *Development* 144: 1988 – 1996

Felipe-Medina N, Gomez HL, Condezo YB, Sanchez-Martin M, Barbero JL, Ramos I, Llano E, Pendas AM (2019) Ubiquitin-specific protease 26 (USP26) is not essential for mouse gametogenesis and fertility. *Chromosoma* 128: 237 – 247

Groth KA, Skakkebaek A, Host C, Gravholt CH, Bojesen A (2013) Clinical review: Klinefelter syndrome–a clinical update. *J Clin Endocrinol Metab* 98: 20 – 30

Guiraldelli MF, Felberg A, Almeida LP, Parikh A, de Castro RO, Pezza RJ (2018) SHOC1 is a ERCC4-(HhH)(2)-like protein, integral to the formation of crossover recombination intermediates during mammalian meiosis. *Plos Genet* 14: e1007381

Harvey J, Jacobs PA, Hassold T, Pettay D (1991) The parental origin of 47, Xxy males. *Birth Def* 26: 289 – 296

Hassold TJ, Sherman SL, Pettay D, Page DC, Jacobs PA (1991) Xy-chromosome nondisjunction in man is associated with diminished recombination in the pseudoautosomal region. *Am J Hum Genet* 49: 253 – 260

Hassold T, Hunt P (2001) To err (meiotically) is human: the genesis of human aneuploidy. *Nat Rev Genet* 2: 280 – 291

Hess RA, Renato de Franca L (2008) Spermatogenesis and cycle of the seminiferous epithelium. *Adv Exp Med Biol* 636: 1 – 15

Jacobs PA, Strong JA (1959) Case of human intersexuality having a possible Xxy sex-determining mechanism. *Nature* 183: 302 – 303

Kauppi L, Barchi M, Baudat F, Romanienko PJ, Keeney S, Jasin M (2011) Distinct properties of the XY pseudoautosomal region crucial for male meiosis. *Science* 331: 916 – 920

Kit Leng Lui S, Iyengar PV, Jaynes P, Isa Z, Pang B, Tan TZ, Eichhorn PJA (2017) USP26 regulates TGF-beta signaling by deubiquitinating and stabilizing SMAD7. *EMBO Rep* 18: 797 – 808

Lahav-Baratz S, Kravtsova-Ivantsiv Y, Golan S, Ciechanover A (2017) The testis-specific USP26 is a deubiquitinating enzyme of the ubiquitin ligase Mdm2. *Biochem Biophys Res Commun* 482: 106 – 111

Lanfranco F, Kamischke A, Zitzmann M, Nieschlag E (2004) Klinefelter's syndrome. *Lancet* 364: 273 – 283

Lowe X, Eskenazi B, Nelson DO, Kidd S, Alme A, Wyrobek AJ (2001) Frequency of XY sperm increases with age in fathers of boys with Klinefelter syndrome. *Am J Hum Genet* 69: 1046 – 1054

Lu LY, Xiong Y, Kuang H, Korakavi G, Yu X (2013) Regulation of the DNA damage response on male meiotic sex chromosomes. *Nat Commun* 4: 2105

Lu LY, Yu XC (2015) Double-strand break repair on sex chromosomes: challenges during male meiotic prophase. *Cell Cycle* 14: 516 – 525

Luddi A, Crifasi L, Quagliarello A, Governini L, De Leo V, Piomboni P (2016) Single nucleotide polymorphisms of USP26 in azoospermic men. *Syst Biol Reprod Med* 62: 372 – 378

Ma Q, Li YC, Guo H, Li CL, Chen JB, Luo ML, Jiang ZM, Li HG, Gui YT (2016) A novel missense mutation in USP26 gene is associated with nonobstructive azoospermia. *Reprod Sci* 23: 1434 – 1441

Moens PB, Kolas NK, Tarsounas M, Marcon E, Cohen PE, Spyropoulos B (2002) The time course and chromosomal localization of recombination-related proteins at meiosis in the mouse are compatible with models that can resolve the early DNA-DNA interactions without reciprocal recombination. *J Cell Sci* 115: 1611 – 1622

 © 2021 The Authors

Neale MJ, Keeney S (2006) Clarifying the mechanics of DNA strand exchange in meiotic recombination. *Nature* 442: 153 – 158

Nicolaidis P, Petersen MB (1998) Origin and mechanisms of non-disjunction in human autosomal trisomies. *Hum Reprod* 13: 313 – 319

Ning B, Zhao W, Qian C, Liu PH, Li QT, Li WY, Wang RF (2017) USP26 functions as a negative regulator of cellular reprogramming by stabilising PRC1 complex components. *Nat Commun* 8: 349

Raudsepp T, Das PJ, Avila F, Chowdhary BP (2012) The pseudoautosomal region and sex chromosome aneuploidies in domestic species. *Sex Dev* 6: 72 – 83

Sakai K, Ito C, Wakabayashi M, Kanzaki S, Ito T, Takada S, Toshimori K, Sekita Y, Kimura T (2019) Usp26 mutation in mice leads to defective spermatogenesis depending on genetic background. *Sci Rep* 9: 13757

Seo JT, Park YS, Lee JS (2004) Successful testicular sperm extraction in Korean Klinefelter syndrome. *Urology* 64: 1208 – 1211

Sha YW, Zheng LK, Ji ZY, Mei LB, Ding L, Lin SB, Wang X, Yang XY, Li P (2018) A novel TEX11 mutation induces azoospermia: a case report of infertile brothers and literature review. *Bmc Med Genet* 19: 63

Skuse D, Printzlau F, Wolstencroft J (2018) Sex chromosome aneuploidies. *Handb Clin Neurol* 147: 355 – 376

Sun SC, Kim NH (2012) Spindle assembly checkpoint and its regulators in meiosis. *Hum Reprod Update* 18: 60 – 72

Swerdloff RS, Lue Y, Liu PY, Erkkila K, Wang C (2011) Mouse model for men with klinefelter syndrome: a multifaceted fit for a complex disorder. *Acta Paediatr* 100: 892 – 899

Tempest HG (2011) Meiotic recombination errors, the origin of sperm aneuploidy and clinical recommendations. *Syst Biol Reprod Med* 57: 93 – 101

Thomas NS, Collins AR, Hassold TJ, Jacobs PA (2000) A reinvestigation of non-disjunction resulting in 47, XXY males of paternal origin. *Eur J Hum Genet* 8: 805 – 808

Thomas NS, Hassold TJ (2003) Aberrant recombination and the origin of Klinefelter syndrome. *Hum Reprod Update* 9: 309 – 317

Tian H, Huo Y, Zhang J, Ding S, Wang Z, Li H, Wang L, Lu M, Liu S, Qiu S *et al* (2019) Disruption of ubiquitin specific protease 26 gene causes male subfertility associated with spermatogenesis defects in mice dagger. *Biol Reprod* 100: 1118 – 1128

Turner JMA (2007) Meiotic sex chromosome inactivation. *Development* 134: 1823 – 1831

Tuttelmann F, Gromoll J (2010) Novel genetic aspects of Klinefelter's syndrome. *Mol Hum Reprod* 16: 386 – 395

Wang PJ, McCarrey JR, Yang F, Page DC (2001) An abundance of X-linked genes expressed in spermatogonia. *Nat Genet* 27: 422 – 426

Wang HY, Wang ML, Wang HC, Bocker W, Iliakis G (2005) Complex H2AX phosphorylation patterns by multiple kinases including ATM and DNA-PK in human cells exposed to ionizing radiation and treated with kinase inhibitors. *J Cell Physiol* 202: 492 – 502

Wang J, Zhao X, Hong RY (2020) USP26 deubiquitinates androgen receptor (AR) in the maintenance of sperm maturation and spermatogenesis through the androgen receptor signaling pathway. *Adv Clin Exp Med* 29: 1153 – 1160

World Health Organization (2001) [Laboratory manual of the WHO for the examination of human semen and sperm-cervical mucus interaction]. *Ann Ist Super Sanita* 37: 1 – 123, I–XII

Xia JD, Chen J, Han YF, Chen H, Yu W, Chen Y, Dai YT (2014) Association of 370–371insACA, 494T > C, and 1423C > T haplotype in ubiquitin-specific protease 26 gene and male infertility: a meta-analysis. *Asian J Androl* 16: 720 – 724

Yang F, Gell K, van der Heijden GW, Eckardt S, Leu NA, Page DC, Benavente R, Her C, Hoog C, McLaughlin KJ *et al* (2008) Meiotic failure in male mice lacking an X-linked factor. *Genes Dev* 22: 682 – 691

Yang F, Silber S, Leu NA, Oates RD, Marszalek JD, Skaletsky H, Brown LG, Rozen S, Page DC, Wang PJ (2015) TEX11 is mutated in infertile men with azoospermia and regulates genome-wide recombination rates in mouse. *Embo Mol Med* 7: 1198 – 1210

Yatsenko AN, Georgiadis AP, Ropke A, Berman AJ, Jaffe T, Olszewska M, Westernstroer B, Sanfilippo J, Kurpisz M, Rajkovic A *et al* (2015) X-Linked TEX11 mutations, meiotic arrest, and azoospermia in infertile men. *New Engl J Med* 372: 2097 – 2107

Zhang W, Liu T, Mi YJ, Yue LD, Wang JM, Liu DW, Yan J, Tian QB (2015) Evidence from enzymatic and meta-analyses does not support a direct association between USP26 gene variants and male infertility. *Andrology* 3: 271 – 279

Zhong C, Yin Q, Xie Z, Bai MZ, Dong R, Tang W, Xing YH, Zhang HL, Yang SM, Chen LL *et al* (2015) CRISPR-Cas9-mediated genetic screening in mice with haploid embryonic stem cells carrying a guide RNA library (vol 17, pg 221, 2015). *Cell Stem Cell* 17: 247

Zhu F, Liu C, Wang F, Yang X, Zhang J, Wu H, Zhang Z, He X, Zhang Z, Zhou P *et al* (2018) Mutations in PMFBP1 cause acephalic spermatozoa syndrome. *Am J Hum Genet* 103: 188 – 199

© 2021 The Authors